Elaboration and experimental verification of a scaling law for REBCO coated conductors based on the physics of pinning

G. Succi

CERN and University of Southampton

This work is described in: [1] G. Succi, A. Ballarino, S. C. Hopkins, C. Barth, Y. Yang, *IEEE Trans. Appl. Supercond.*, vol. 34, no. 3, 2024.

Outline

- REBCO properties and manufacturing routes
- Scaling laws
- Experimental activities
- Angular scaling
- Conclusions and next steps

Outline

- REBCO properties and manufacturing routes
- Scaling laws
- Experimental activities
- Angular scaling
- Conclusions and next steps

Introduction

Why do we need scaling laws?

- Design and modelling of coils and other devices wound with REBCO tapes requires precise knowledge of their electrical properties.

- REBCO is anisotropic and characterized by $I_c = I_c(B, T, \theta)$.

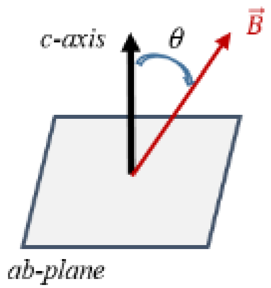

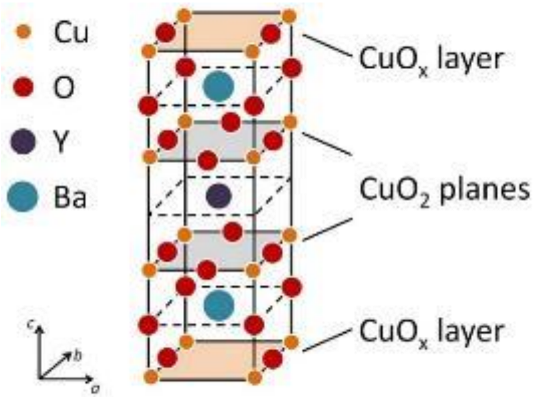

reproduced from [2]

- *Scaling laws* describe tape properties over the full range of B, T, θ with much lesser burden compared to a thorough experimental campaign.

[2] E. Stilp et al., *Scientific reports*, 2014.

Challenges of the REBCO material – 1/4

1) REBCO ($RE_1Ba_2Cu_3O_{7-\delta}$) is a *quaternary system* and its oxygen stoichiometry has a decisive impact on its functional properties, which are strongly anisotropic.

2) The coherence length, ξ, is very low for REBCO, causing the grain boundaries to be connected by weak links → pinning defects must be of the nanoscale size to not block the current transport through the grain boundaries.

Superconductor	$T_{c,0}$ [K]	$B_{c2,0}$ [T]	ξ [nm]
Nb-Ti	9.5	14.5	5
Nb_3Sn	18.3	28-30	3-4
MgB_2	39	32	3-4
REBCO	90	150	1-2
BSCCO-2223	110	150	1-2

reproduced from [3], [4]

In addition, pinning defects must not disrupt the superconducting planes.

[3] M. Cyrot and D. Pavuna, *Introduction to superconductivity and high-T_c materials*, 1992.
[4] A. Ballarino, *CAS on Normal and Superconducting Magnets*, 2023.

Challenges of the REBCO material – 2/4

3) The anisotropic crystalline lattice of REBCO induces much better electrical conduction along the *ab*-planes than along the *c*-axis (**mass anisotropy**)

Material inclusions improve the electrical properties:

Uncorrelated (random) defects enhance conduction at all angles

Correlated defects (e.g. twin boundaries and dislocations) enhance conduction at specific angles.

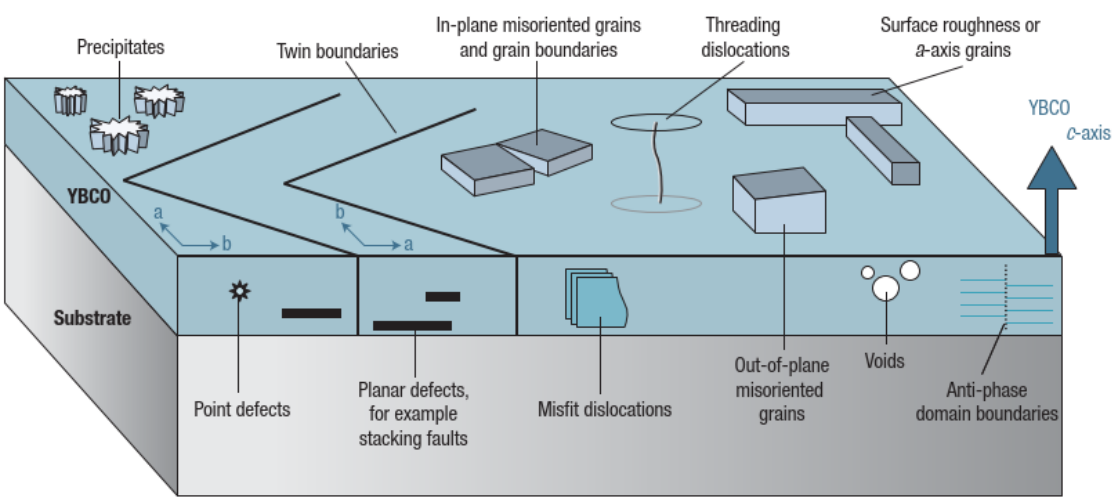

reproduced from [5]

Challenges of the REBCO material – 3/4

3) The anisotropic crystalline lattice of REBCO induces much better electrical conduction along the *ab*-planes than along the *c*-axis (**mass anisotropy**)

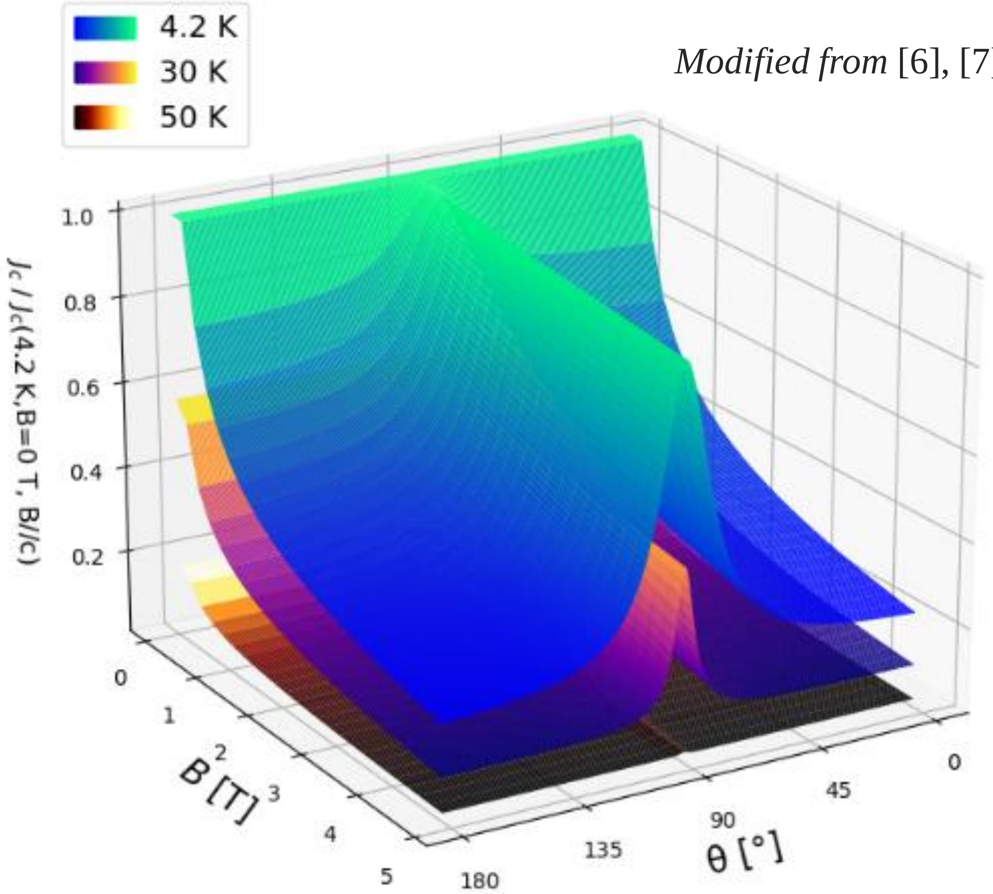

Modified from [6], [7]

[6] J. Fleiter and A. Ballarino, *CERN EDMS document no. 1426239*, 2014.
[7] J. van Nugteren, *PhD thesis*, *Twente University*, 2016.

Challenges of the REBCO material – 4/4

4) Superconductivity acts along 2D planes in REBCO, causing *poor electronic transport perpendicular to the planes* → Very high grain alignment is required to permit current transfer along the conductor length.

5) Because of these reasons, REBCO conductors must be manufactured by **epitaxial thin film growth** on a flexible substrate.

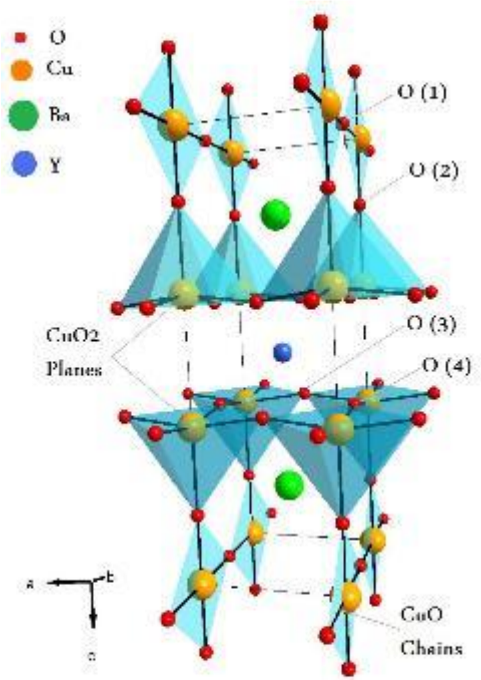

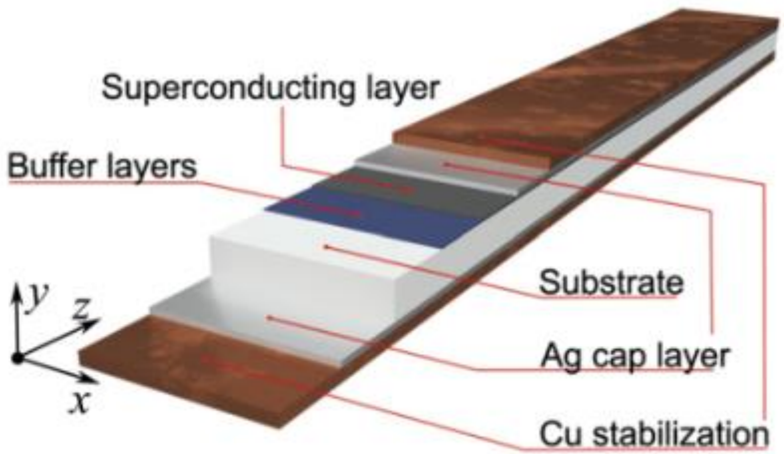

reproduced from [8]

Tape architecture and manufacturing routes

Two main manufacturing methods can be adopted:

1) *Substrate*: Hastelloy C-276 because of its non-magnetic character, strength, and ductility under stress.

   Buffer layers: textured $MgO + Al_2O_3$ and other oxides, for interfacing the substrate with the REBCO. Texturing is provided by Ion Beam Assisted Deposition (IBAD).

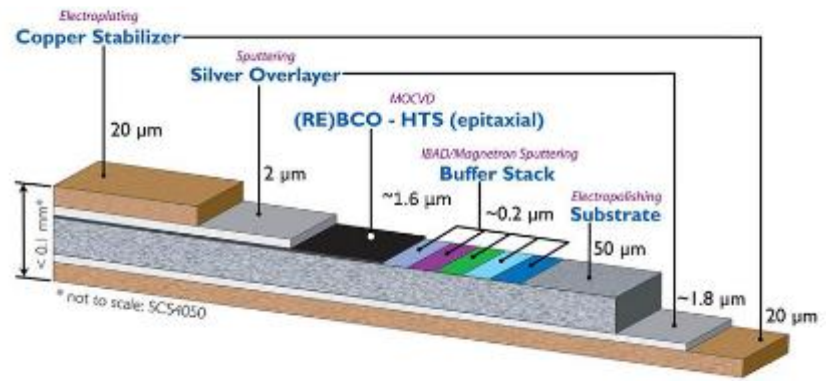

   Chemical deposition, e.g. Metal Organic Deposition (MOD), Metal Organic Chemical Vapour Deposition (MOCVD), or **Physical deposition**, e.g. Pulsed Laser Deposition (PLD) or Reactive Co-Evaporation (RCE)

   → The achieved grain misorientation is 2-3°, comparable to the growth on single-crystal substrates.

2) Rolling-Assisted Biaxially Textured Substrate (RABiTS) of a Ni-W substrate to achieve a 5° - 7° grain misorientation, followed by solution deposition and thermal processing for crystallization.

Application regimes and Supersaturation

- Three regions can be identified in the $I_c(B,T)$ diagram based on applications.
- Each one is characterized by the nature of the defects and the processing leading to it.

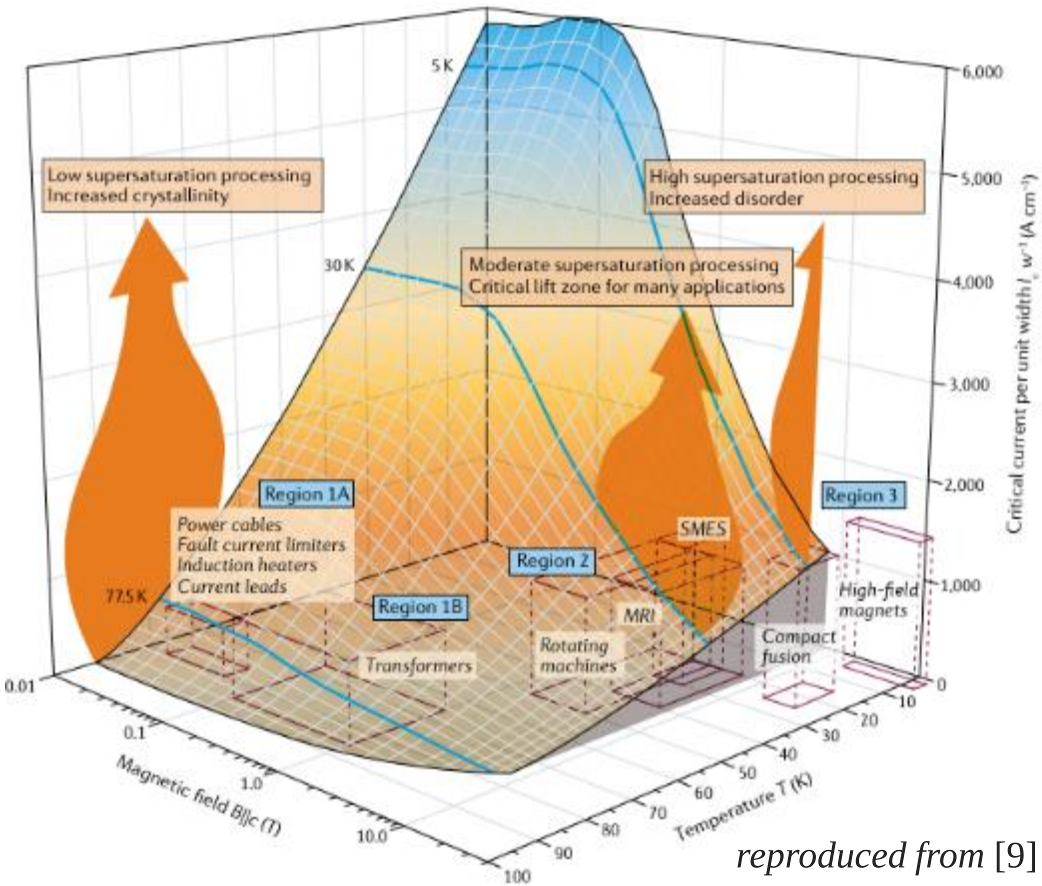

reproduced from [9]

Region	Temperature	Field
1A	65 - 77 K	<0.1 T
1B	65 - 77 K	0.1 - 1 T
2	20 - 40 K	>1 T
3	<20 K	>10 T

Application regimes and Supersaturation

- The degree of **supersaturation** identifies the *concentration of the REBCO chemical species above the equilibrium level*. It is also linked to the kinetics of film growth.

Region 1A (65 - 77 K, < 0.1 T). High I_c is achieved by highly crystalline grains with few pinning defects.

Region 1B (65 - 77 K, 0.1 - 1 T). Pinning is difficult because of thermal activation occurring at these high T levels. Ideal for transformers.

→ Low supersaturation

Region 2 (20 – 40 K, >1 T). The requirement for achieving high performance is to have a complex pinning landscape. Ideal for rotating machines.

→ Moderate supersaturation

Region 3 (<10 K, >10 T). A high density of point defects is required to pin the high number of flux lines penetrating in the material resulting from the high field levels.

→ High supersaturation

High T_c = High T_{op}?

- REBCO has a critical temperature, T_c, of about 90 K.

- Ideally, one would want to operate in liquid nitrogen, LN2, down to 65 K, while carrying high transport currents in moderate fields. However, this is not achievable in practice, since it is not possible to pin the flux vortices against the Lorentz force arising from the combined action of current and field.

⇩

- Lower operating temperatures are required to provide a deep pinning potential through the increased condensation energy of the superconductor.

- This, of course, contrasts with the cryogenic efficiency of devices (Carnot):

  - *3 W/W*, at 77 K
  - *70 W/W*, at 4.2 K

→ The best option is to operate at around 20 – 30 K using electrical cooling.

Present-day performance and the need for a scaling law

At present, the performance of coated conductors has reached record values of [10]:

- $J_{c,eng}(4.2\text{ K}, 20\text{ T}) = 2000\ A/mm^2$
- $J_{c,eng}(20\text{ K}, 20\text{ T}) = 1000\ A/mm^2$
- $J_{c,eng}(77\text{ K, s.f.}) > 600\ A/mm^2$

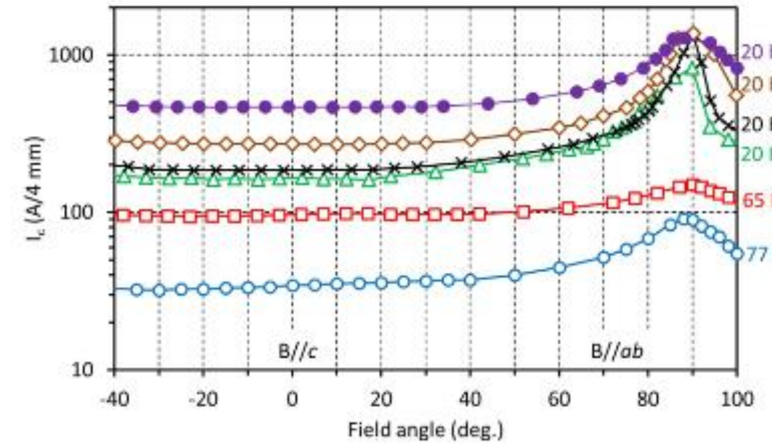

However, a *full* magnetic field, temperature, and angular dependence of the I_c is lacking, unlike for Nb-Ti and Nb_3Sn [11], [12].

$$J_c = \frac{C_0}{B}\, b^{\alpha}\,(1-b)^{\beta}\,(1-t^{n})^{\gamma}$$

$$b = \frac{B}{B_{c,2}} \qquad t = \frac{T}{T_{c,0}}$$

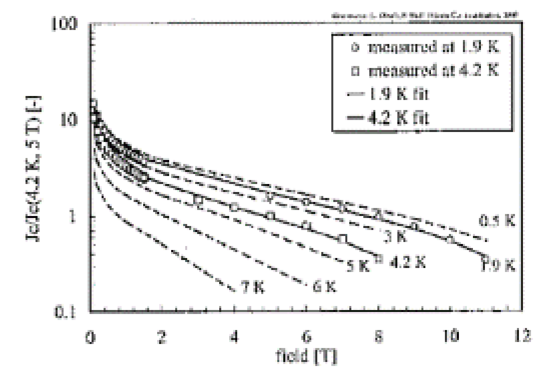

Fig. 7. Field dependence of the normalized $J_c(B,T)$ / J_c (5 T, 4.2 K) for a typical LHC strand [13]-[14], measured at 1.9 and 4.2 K. The fit to the data is shown (solid lines) together with curves generated for different temperatures (dashed lines).

[10] A. Molodyk et al., *Sci. Rep.*, vol. 11, 2021.
[11] E. J. Kramer, *J. Appl. Phys.*, 1973.
[12] L. Bottura, IEEE Trans. Appl. Supercond., 2000.

Outline

- REBCO properties and manufacturing routes
- Scaling laws
- Experimental activities
- Angular scaling
- Conclusions and next steps

Phenomenology and physical interpretation - 1/2

The $I_c(B)$ dependence is the combination of *3 regions* in a log-log plot [13], [14].

$J_c(B, B//c)$ for various T levels - SP tape - Xu et al. (2012) *modified from* [13]

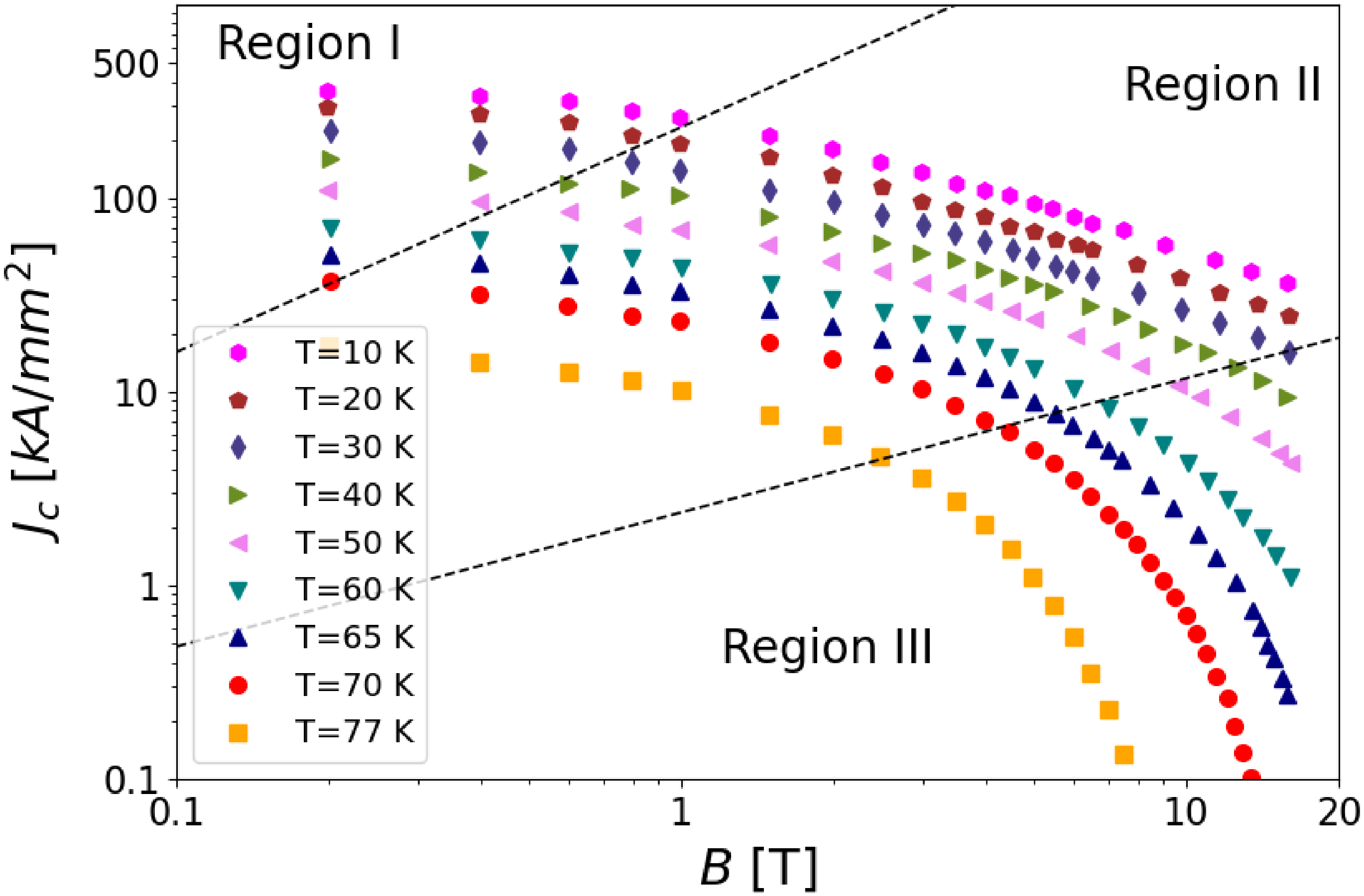

[13] A. Xu et al., *Physical Review B*, 2012.

[14] C. Senatore et al., *Supercond. Sci. Techn.*, 2016.

Phenomenology and physical interpretation - 2/2

Region I: Single vortex pinning regime

Vortices barely interact with each other in *Region I*, as their density is much lower than the density of the pinning centres.

⇨ I_c is field independent, or $I_{c,0} = I_{c,0}(T)$.

Region II: Collective pinning regime

J_c is controlled by the collective pinning of vortex bundles confined in a fixed volume, and it is thus field dependent.

⇨ Starts at $B_0 = B_0(T)$, the *kink* field

Region III: Thermal activation regime

The Lorentz force de-pins all weak pinning centres (0-D defects), leaving only strong centres (1-D columnar defects, much lower in density).

From intermediate temperatures (30 K – 40 K), thermal activation also contributes to depin the vortices.

⇨ Further decrease in performance from $B \approx 0.35 – 0.4\ B_{irr}$.

Past attempts at scaling laws – 1/2

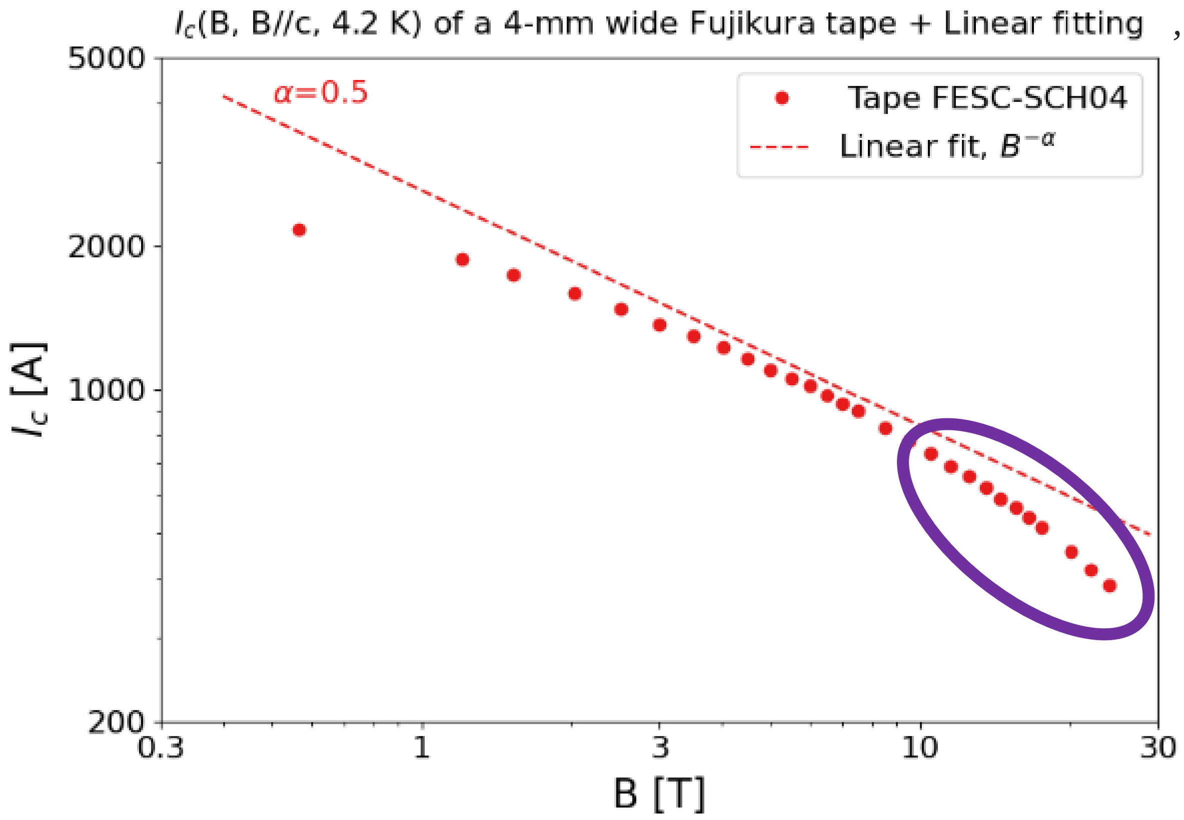

, *modified from* [15]

- The scaling [13, 14]:

$$I_c \propto B^{-\alpha}$$

is valid over *Region II* (3 T < B < 10 T).

- **Extending to high fields**, *Region III* [6, 7]:

$$I_c(B) = \frac{\alpha}{B} \cdot b^p \cdot (1-b)^q$$

$b = \frac{B}{B_{irr}}$, reduced field

α, p, q fitting parameters

This expression remains valid down to ~ 0.5 T - 1 T.

[6] J. Fleiter and A. Ballarino, *CERN EDMS no. 1426239*, 2014.
[7] J. van Nugteren, *PhD thesis*, 2016.
[14] C. Senatore et al., *Supercond. Sci. Techn.*, 2016.
[15] M. Daibo, “Recent progress at Fujikura”, 2019.

Past attempts at scaling laws – 2/2

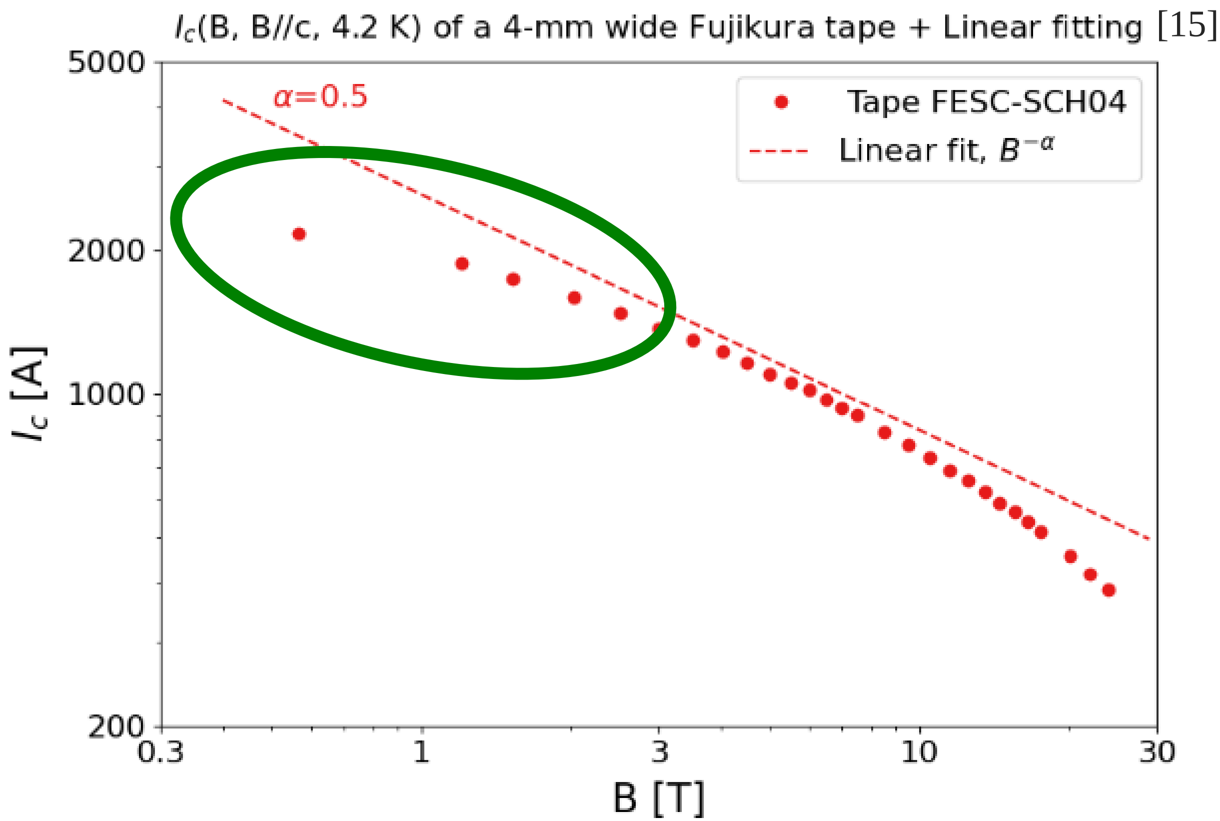

- The scaling [13, 14]:

$$I_c \propto B^{-\alpha}$$

is valid over *Region II* (3 T < B < 10 T).

- **Extending to low fields**, *Region I*:
  1) *Elaborate the effect of self-field on the I_c*
  2) *Compute magnetization effects at low fields*

The proposed scaling law $I_c(B)$ - 1/5

- $I_c = I_{c,0} \cdot B^{-\alpha}$
- $I_c = I_{c,0} \cdot \frac{\gamma}{B} \left(\frac{B}{B_{irr}}\right)^p \cdot \left(1 - \frac{B}{B_{irr}}\right)^q$

Parameter	Value
$I_{c,0}$	2000 A
α	0.5
γ	10 T
p	0.5
q	2.0
B_{irr}	100 T

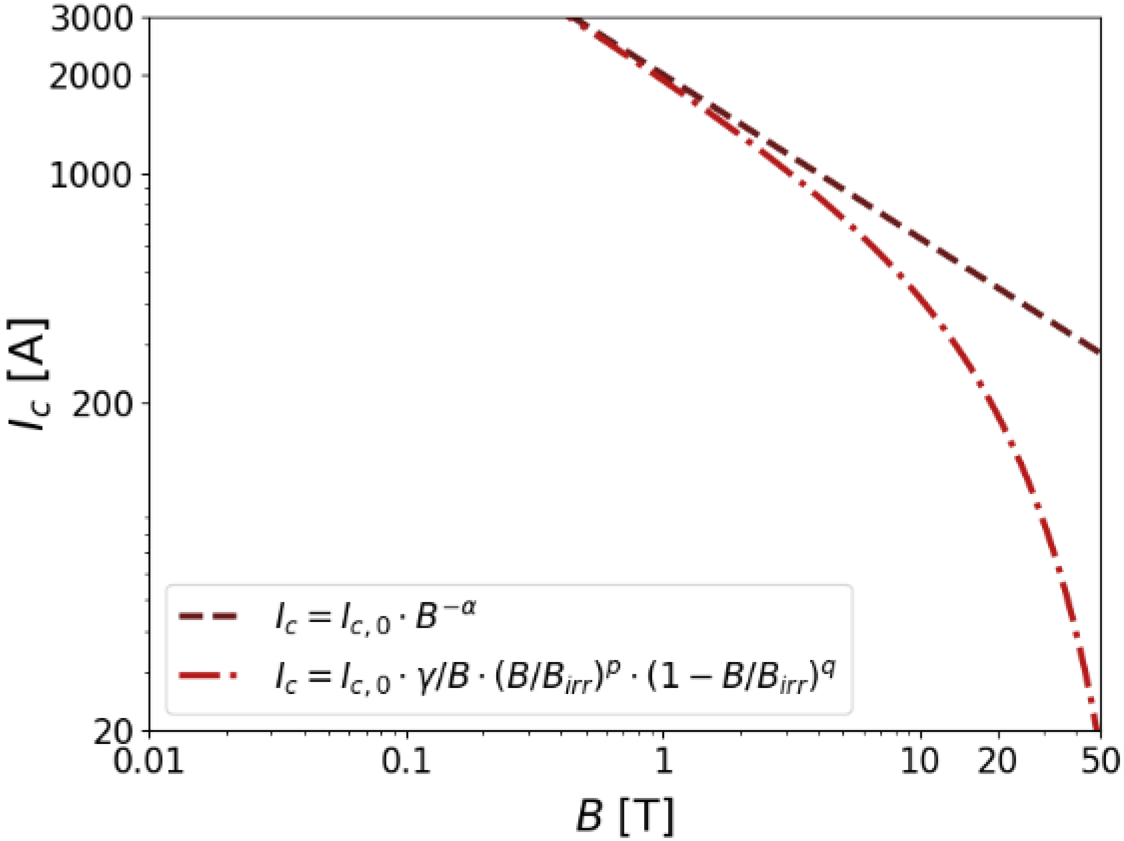

The proposed scaling law $I_c(B)$ - 2/5

$$F_p = J_c(B) \cdot B \quad ; \qquad J_c(B) = \frac{F_p}{B} \propto b^{p-1} \cdot (1-b)^q \quad , \; b = \frac{B}{B_{irr}}$$

- We replace: $b \longrightarrow 1 + \frac{b}{b_0}$ in the first term *only* , $b_0 = \frac{B_0}{B_{irr}}$

B_0 is the kink field, which defines the transition from *Region I* of single vortex pinning, to *Region II* of collective pinning.

We can write $p - 1 = -\alpha$

$$I_c(B, T = T^*, \theta = \theta^*) = \underbrace{I^*_{c,0}}_{\text{Plateau}} \cdot \underbrace{\left(1 + \frac{B}{B^*_0}\right)^{-\alpha^*}}_{\text{Linear decrease}} \cdot \underbrace{\left(1 - \frac{B}{B^*_{irr}}\right)^{q^*}}_{\text{Drop at } B \approx B_{irr}}$$

$$\begin{cases} I^*_{c,0} = I_c(B = 0, T^*) \\ B^*_0 = B_0(T^*, \theta^*) \\ \alpha^* = \alpha^*(T^*, \theta^*) \\ B^*_{irr} = B_{irr}(T^*, \theta^*) \\ q = q(T^*, \theta^*) \end{cases}$$

The proposed scaling law $I_c(B)$ - 3/5

$$I_c(B, T = T^*, \theta = \theta^*) = \underbrace{I_{c,0}^*}_{\text{Plateau}} \cdot \underbrace{\left(1 + \frac{B}{B_0^*}\right)^{-\alpha^*}}_{\text{Linear decrease}} \cdot \underbrace{\left(1 - \frac{B}{B_{irr}^*}\right)^{q^*}}_{\text{Drop at } B \approx B_{irr}}$$

Pinning force - Nb_3Sn [11]

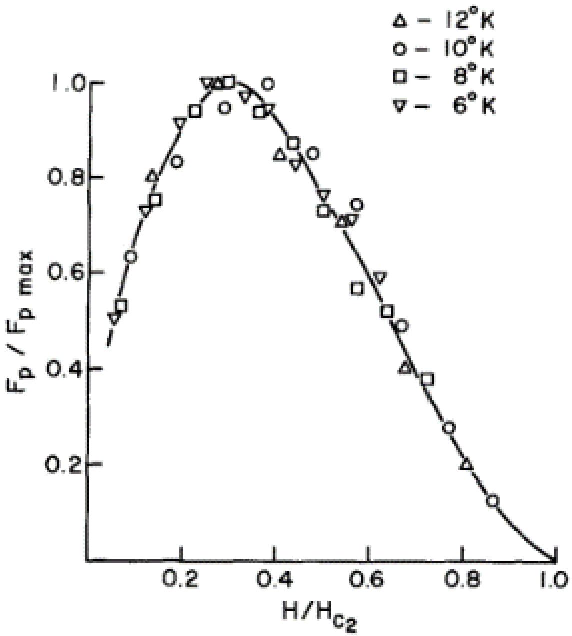

Pinning force - REBCO

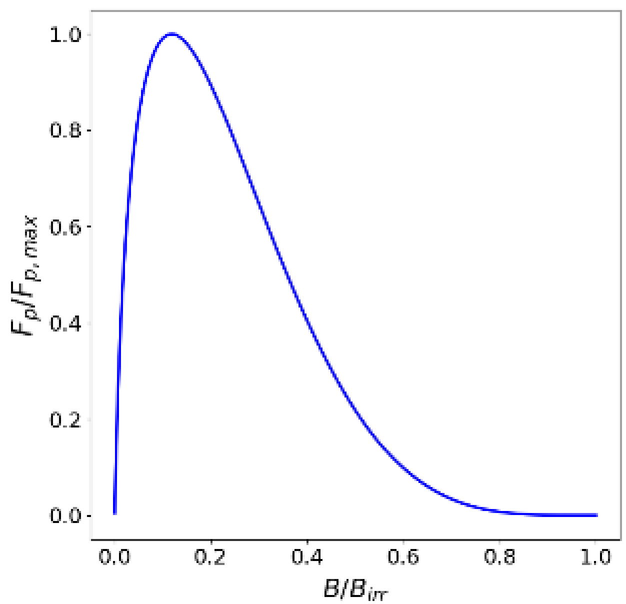

For Nb_3Sn, $F_{p,max} / F_p$ is at 0.3 [11] .

The proposed scaling law suggests that the maximum occurs at B/B_{irr} = 0.12, namely $B \approx$ 18 - 20 T.

The proposed scaling law $I_c(B)$ - 4/5

$$I_c(B, T = T^*, \theta = \theta^*) = \underbrace{I^*_{c,0}}_{\text{Plateau}} \cdot \underbrace{\left(1 + \frac{B}{B^*_0}\right)^{-\alpha^*}}_{\text{Linear decrease}} \cdot \underbrace{\left(1 - \frac{B}{B^*_{irr}}\right)^{q^*}}_{\text{Drop at } B \approx B_{irr}}$$

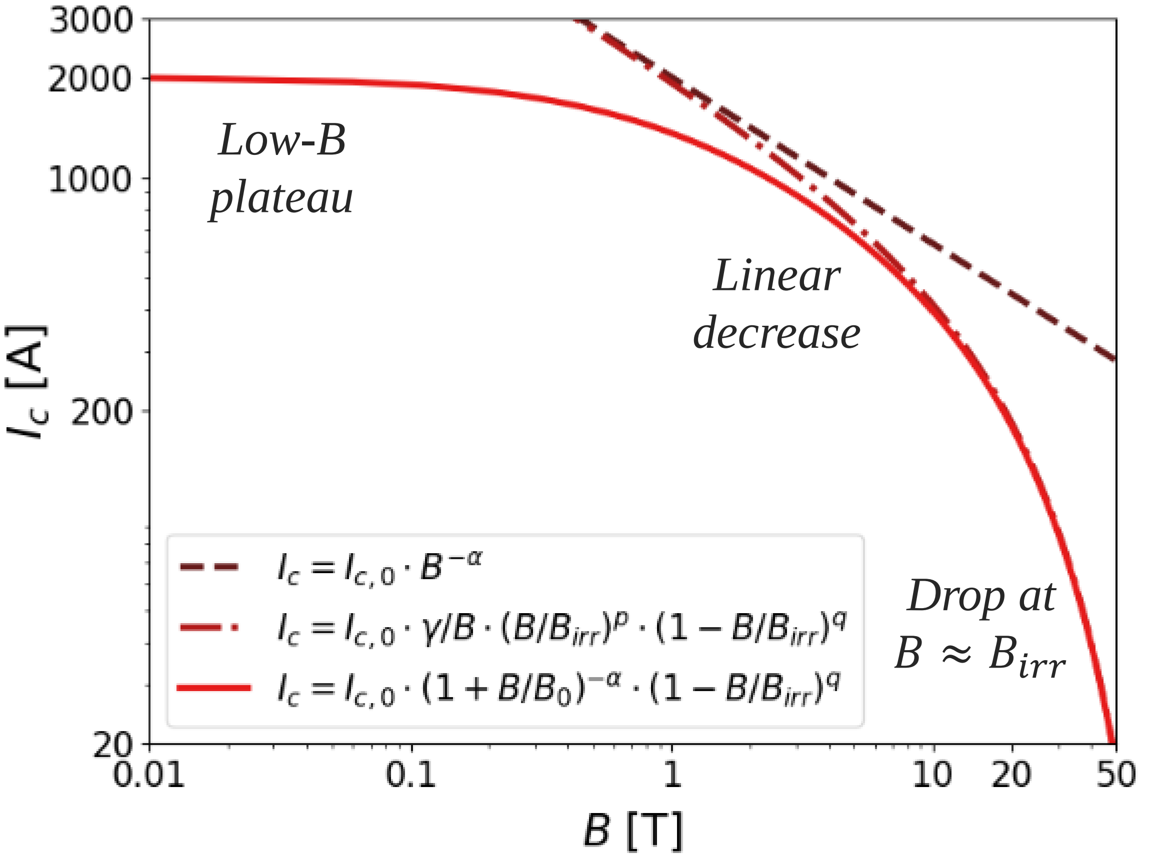

Parameter	Value
$I_{c,0}$	2000 A
α	0.5
γ	10 T
p	0.5
q	2.0
B_{irr}	100 T

The proposed scaling law $I_c(B)$ - 5/5

$$I_c(B, T = T^*, \theta = \theta^*) = I_{c,0}^* \cdot \left(1 + \frac{B}{B_0^*}\right)^{-\alpha^*} \cdot \left(1 - \frac{B}{B_{irr}^*}\right)^{q^*}$$

$$\begin{cases} I_{c,0}^* = I_c(B = 0, T^*) \\ B_0^* = B_0(T^*, \theta^*) \\ \alpha^* = \alpha^*\,(T^*, \theta^*) \\ B_{irr}^* = B_{irr}(T^*, \theta^*) \\ q = q\,(T^*, \theta^*) \end{cases}$$

$J_c(B, B//c)$ for various T levels - SP tape - Xu et al. (2012) , *modified from* [13]

- $B < 0.1$ T: expected plateau

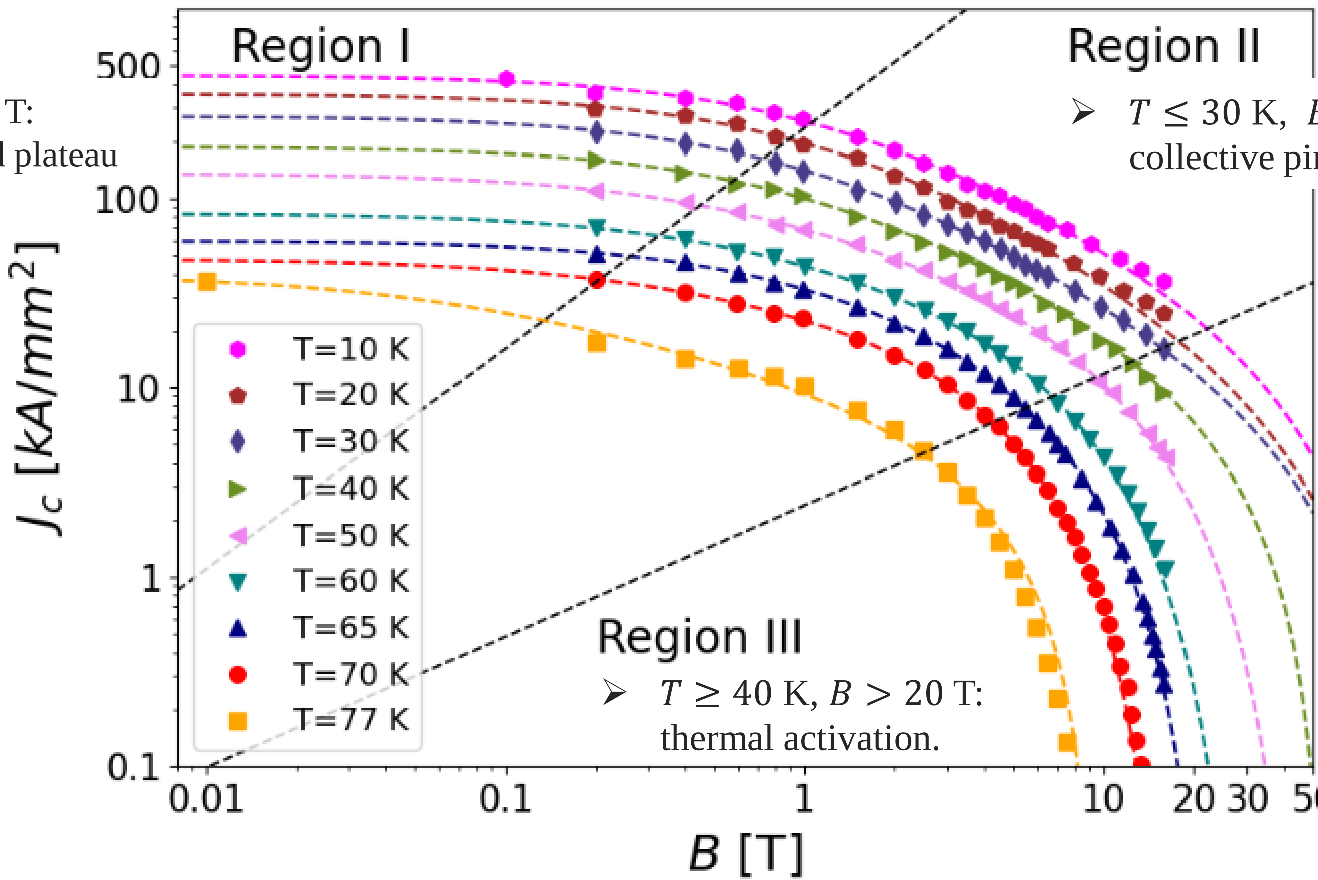

- $T \leq 30$ K, $B < 20$ T: collective pinning only.
- $T \geq 40$ K, $B > 20$ T: thermal activation.

Lack of data at low fields

- Literature measurements are limited in current ≲1.8 kA

  → Need to explore the low-field region (<3 T) where I_c > 2 kA, to *access* the B_0.

$I_c(4.2$ K, $B, B//c)$ - 4 mm, S-Innovations - Molodyk et al. 2021 , *modified from* [10]

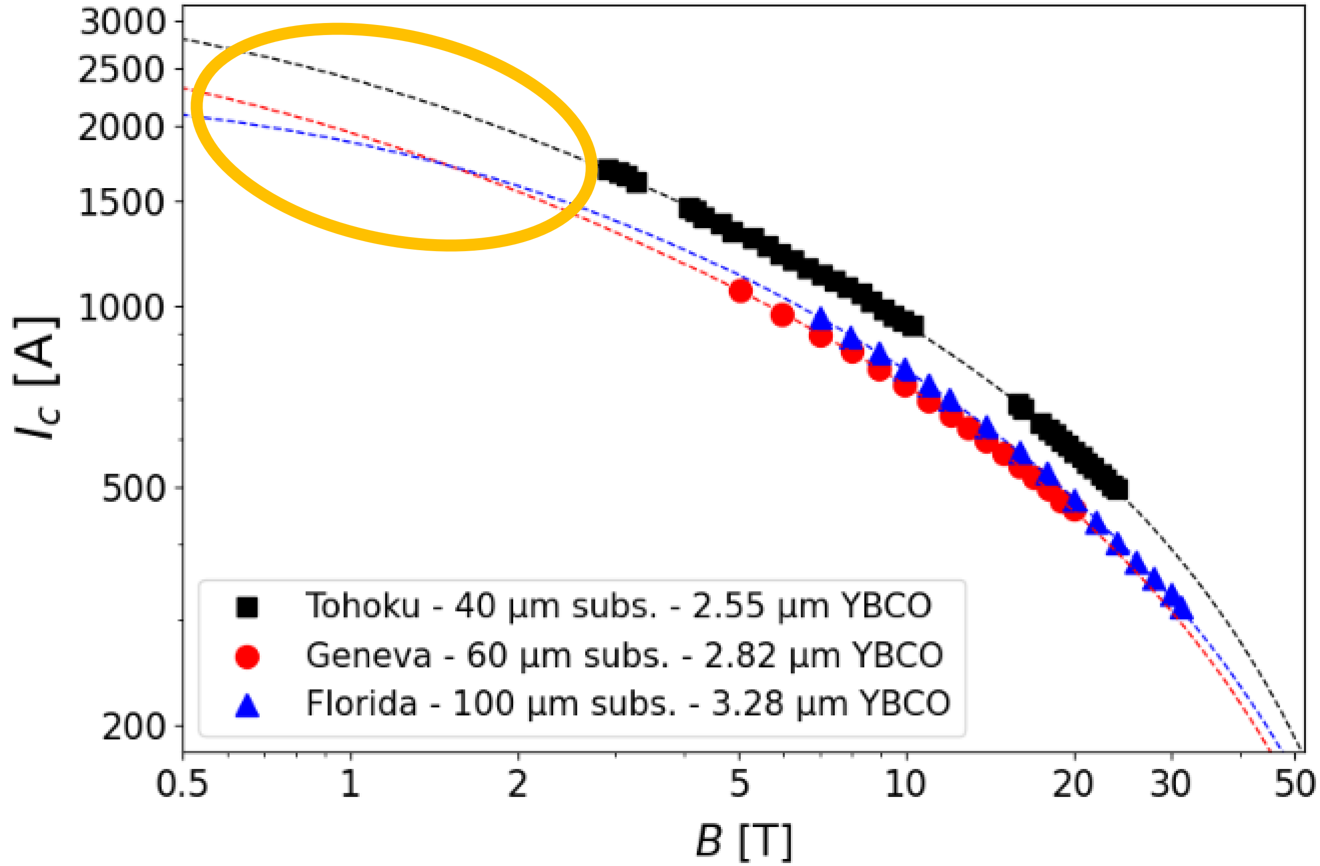

Outline

- REBCO properties and manufacturing routes
- Scaling laws
- Experimental activities
- Angular scaling
- Conclusions and next steps

Transport current – 1/3

➢ **Development of a U-shape sample holder to test I_c(4.2 K, B, $B \perp$ tape)** in a solenoid test station

- Central G10 part to avoid current sharing with the holder
- 15 mm straight region ⊥ background field of the solenoid
- 18 mm bending radius, higher than most tape specs

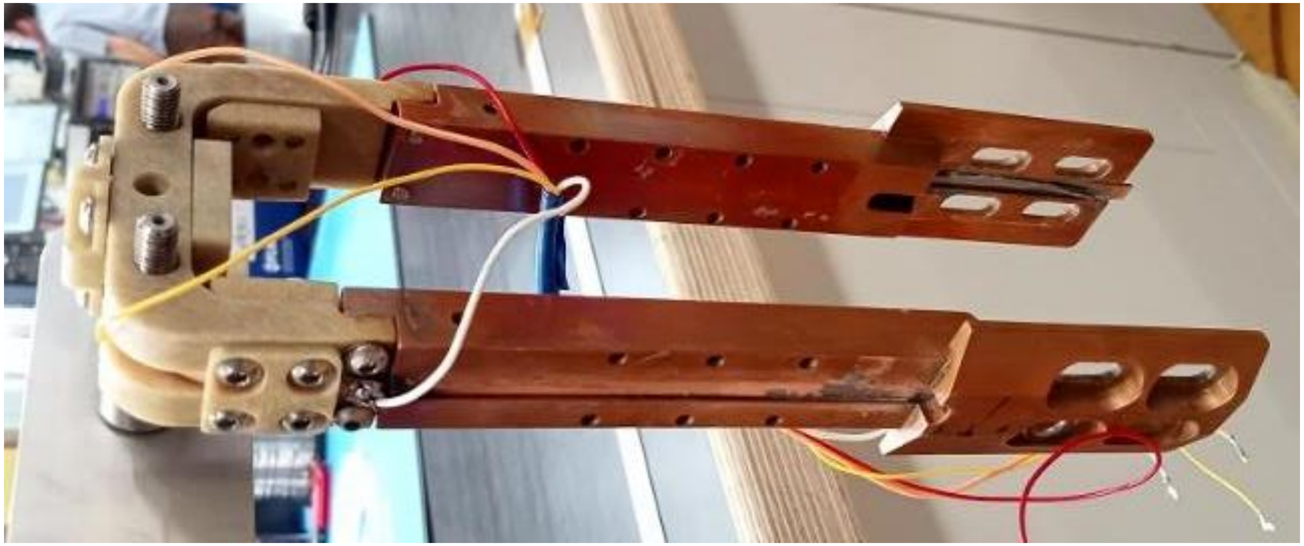

Transport current – 2/3

- *Tape from S-Innovations*

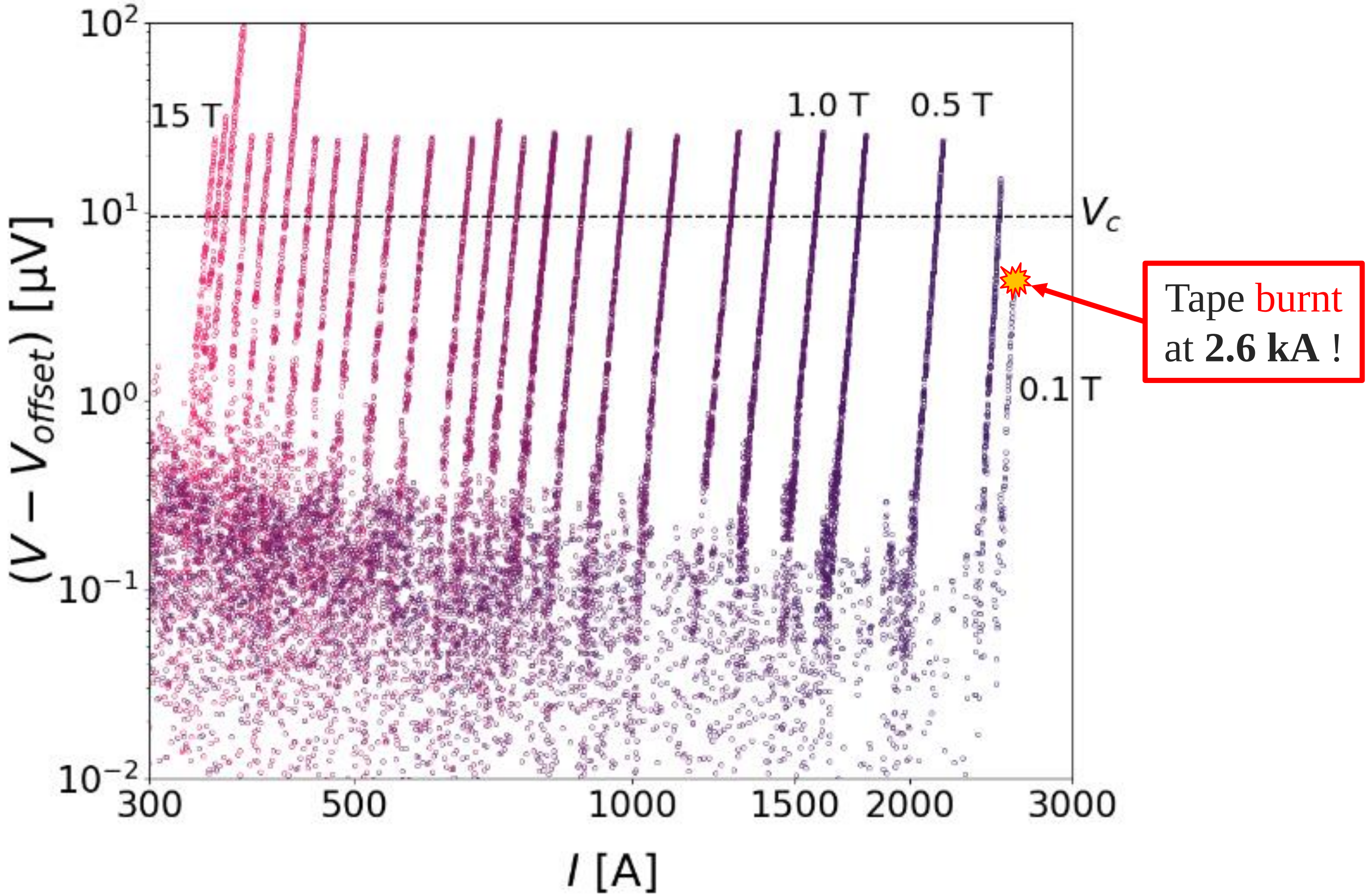

Transport current – 3/3

- *Tape from Faraday Factory*

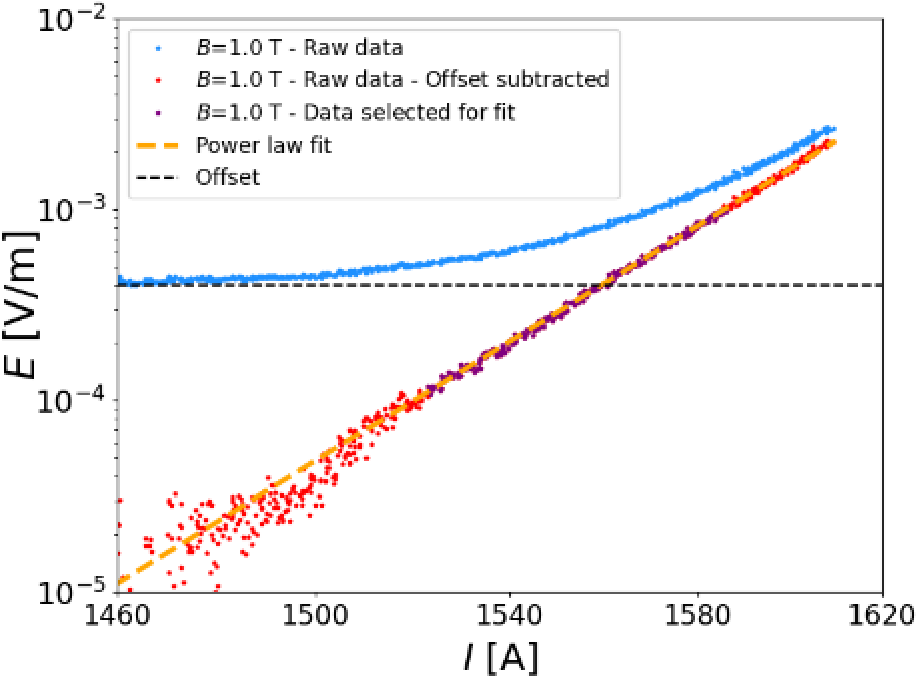

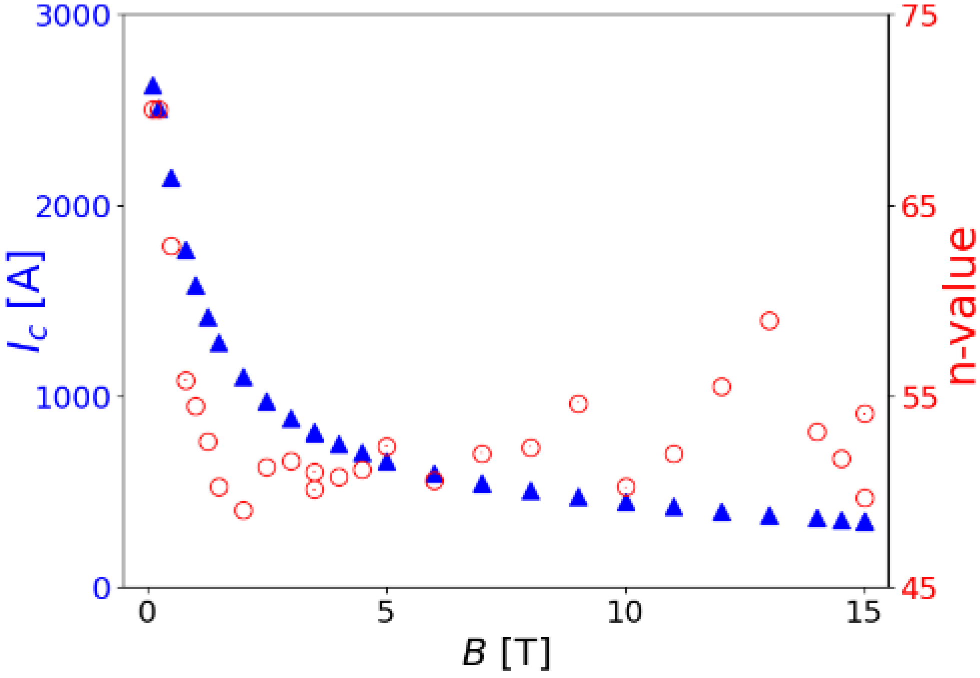

Magnetization – 1/2

- Magnetization measurements in the VSM facility

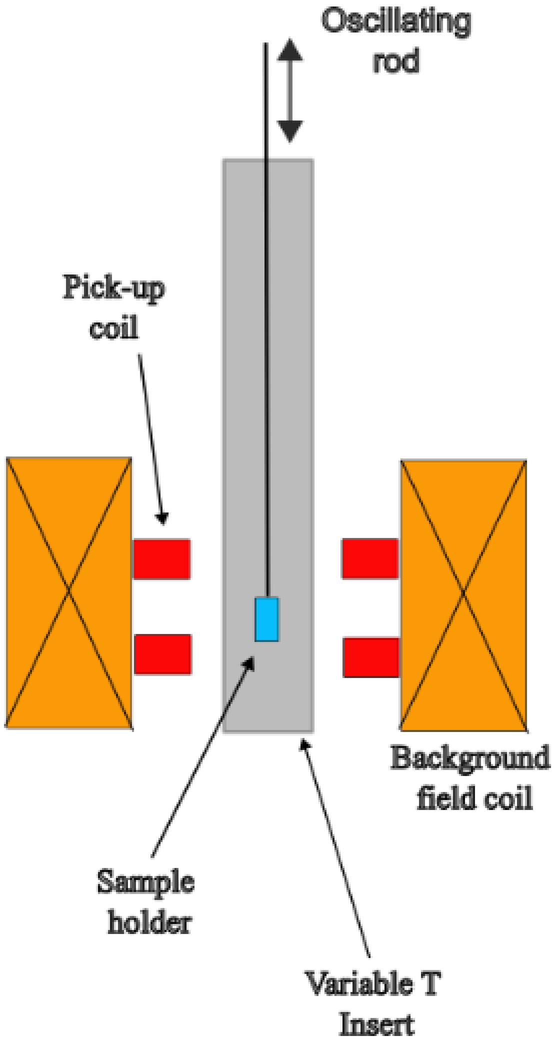

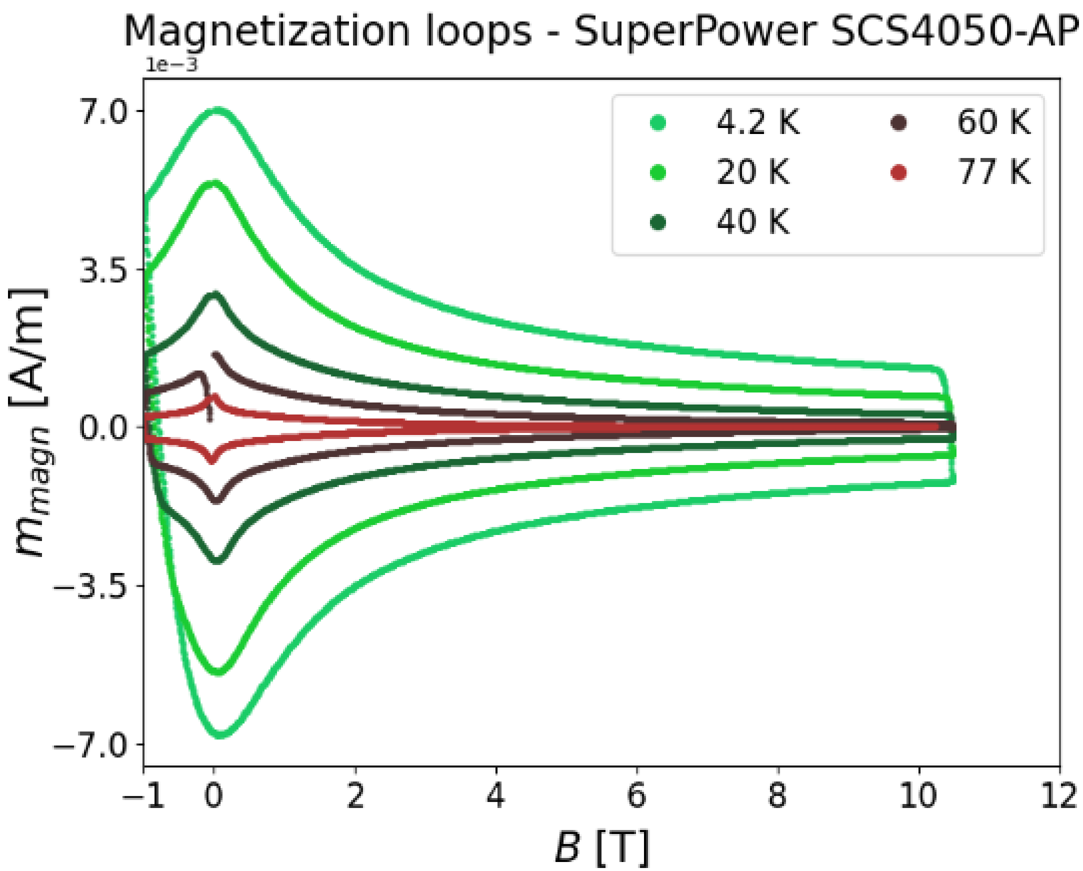

Magnetization – 2/2

- Magnetization measurements in the VSM facility

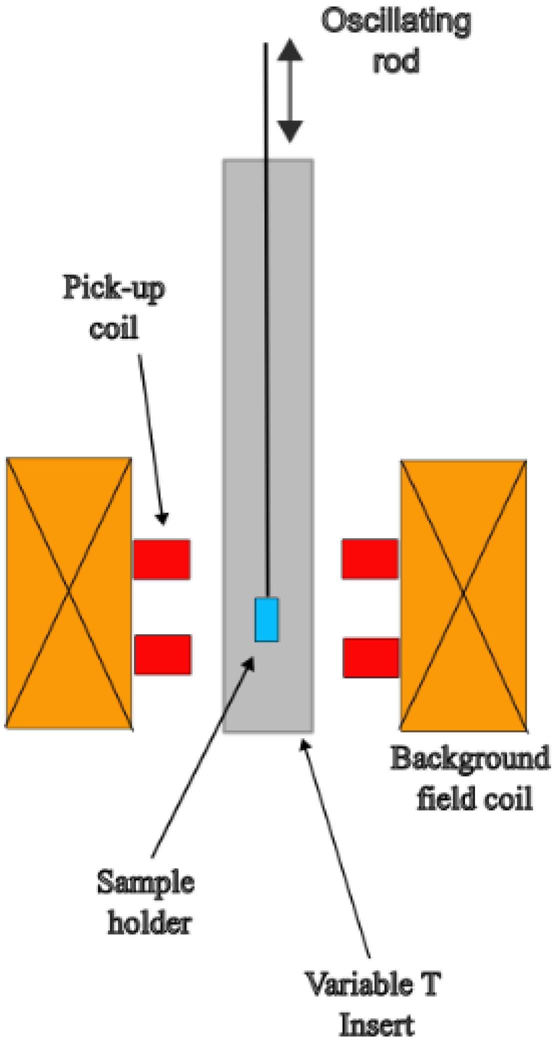

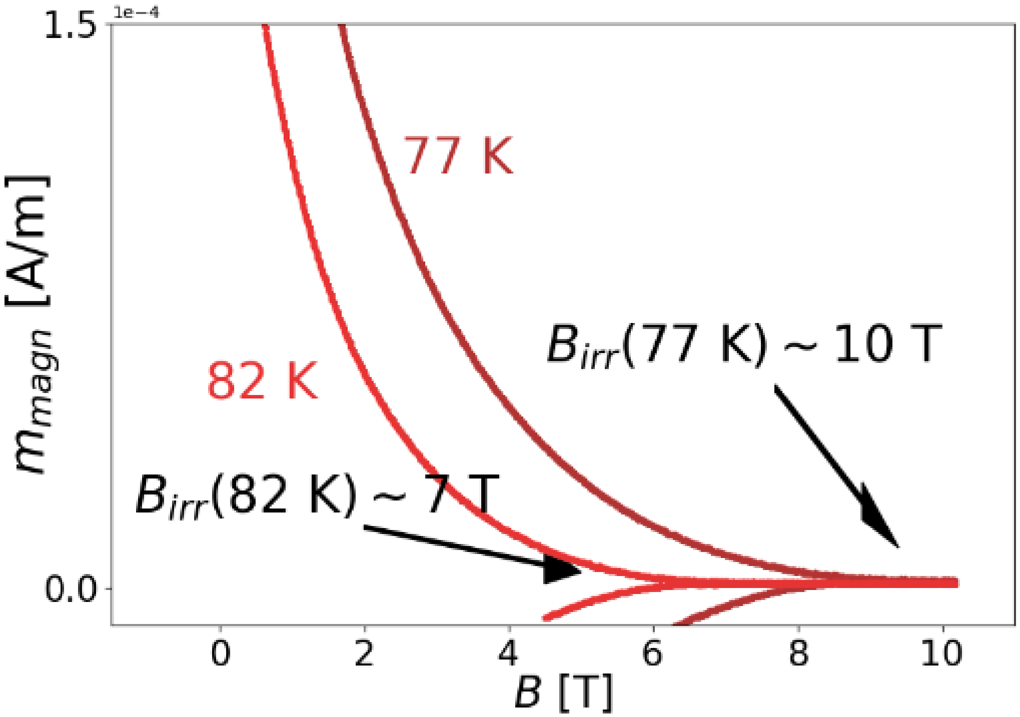

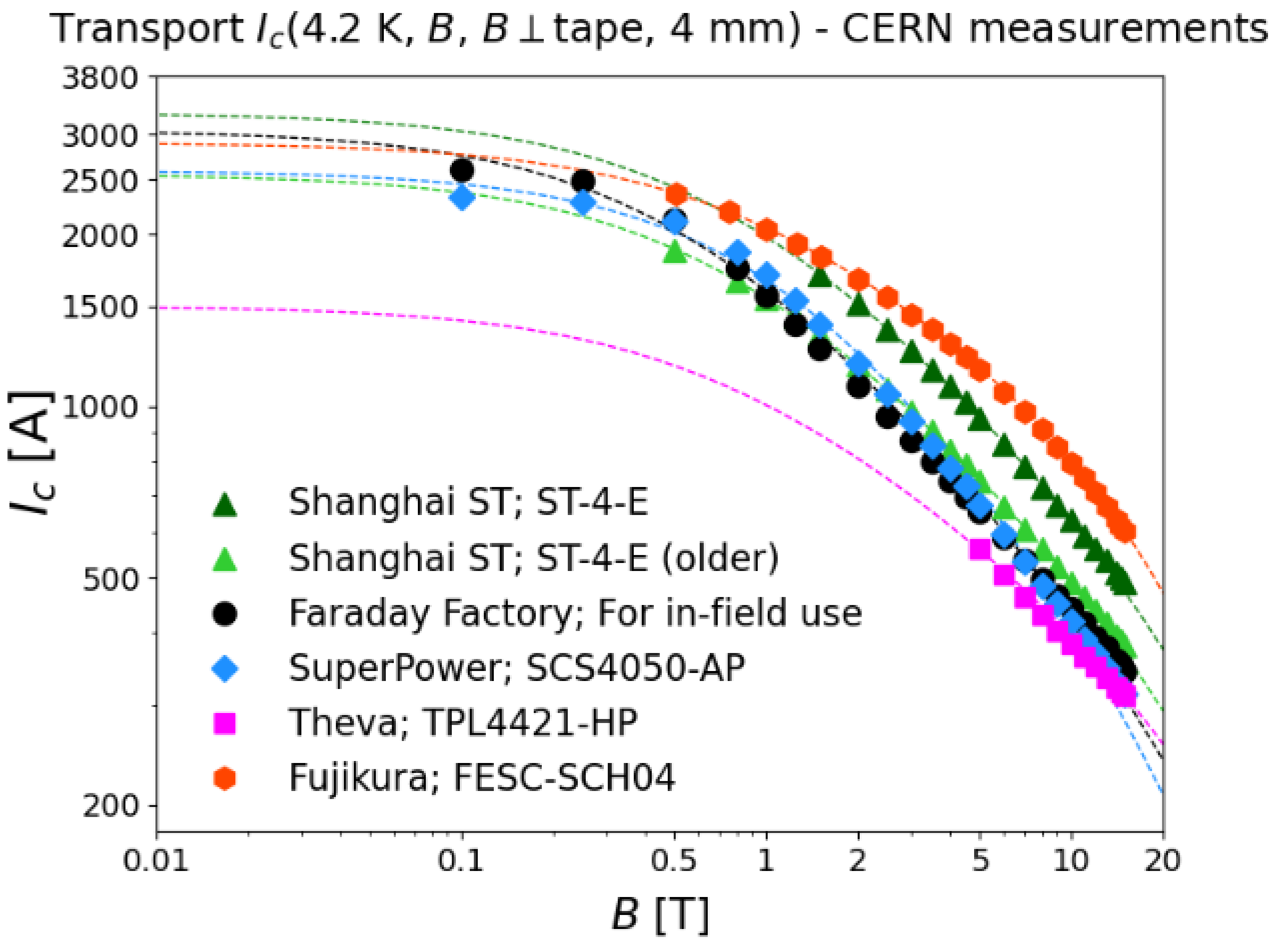

Fitting parameters		$I_{c,0}$	α	B_0	q	B_{irr}
Allowed ranges		<= 3500A	0 - 1	0 - 2 T	2 - 5	0 - 150 T

Manufacturer	Tape type					
Shanghai ST	ST-4-E	3274 A	0.56	0.72 T	2.0	150 T
Shanghai ST	ST-4-E (older)	2553 A	0.56	0.72 T	2.0	150 T
Faraday Factory	For in-field use	3052 A	0.63	0.57 T	2.0	150 T
SuperPower	SCS4050-AP	2593 A	0.84	1.5 T	2.0	150 T
Theva	TPL4421-HP	1500 A	0.44	0.71 T	2.0	150 T
Fujikura	FESC-SCH04	2907 A	0.40	0.81 T	2.0	90 T

Magnetization $I_c(B,T)$ - SP SCS4050-AP - CERN measurements

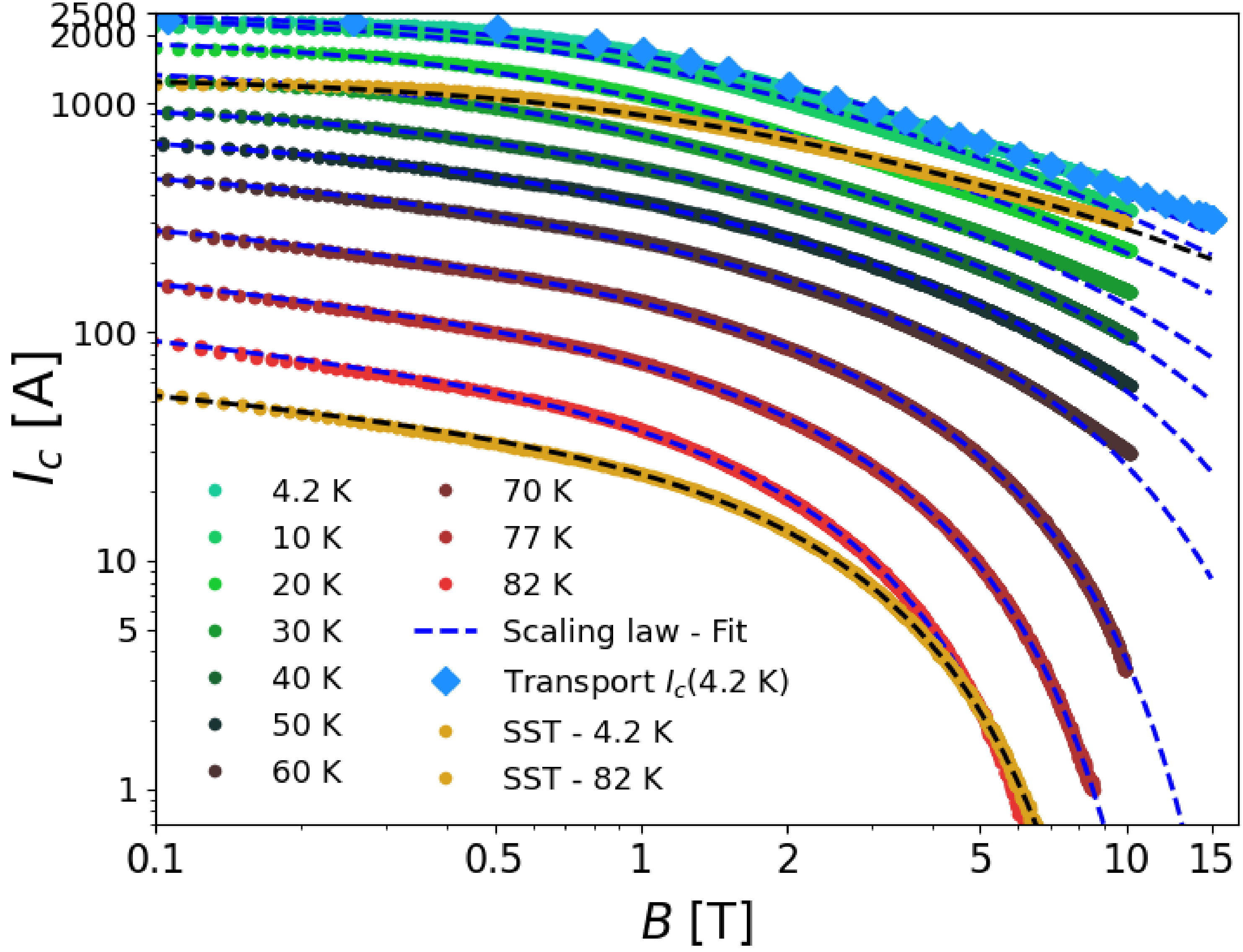

Scaling parameters – Temperature dependence

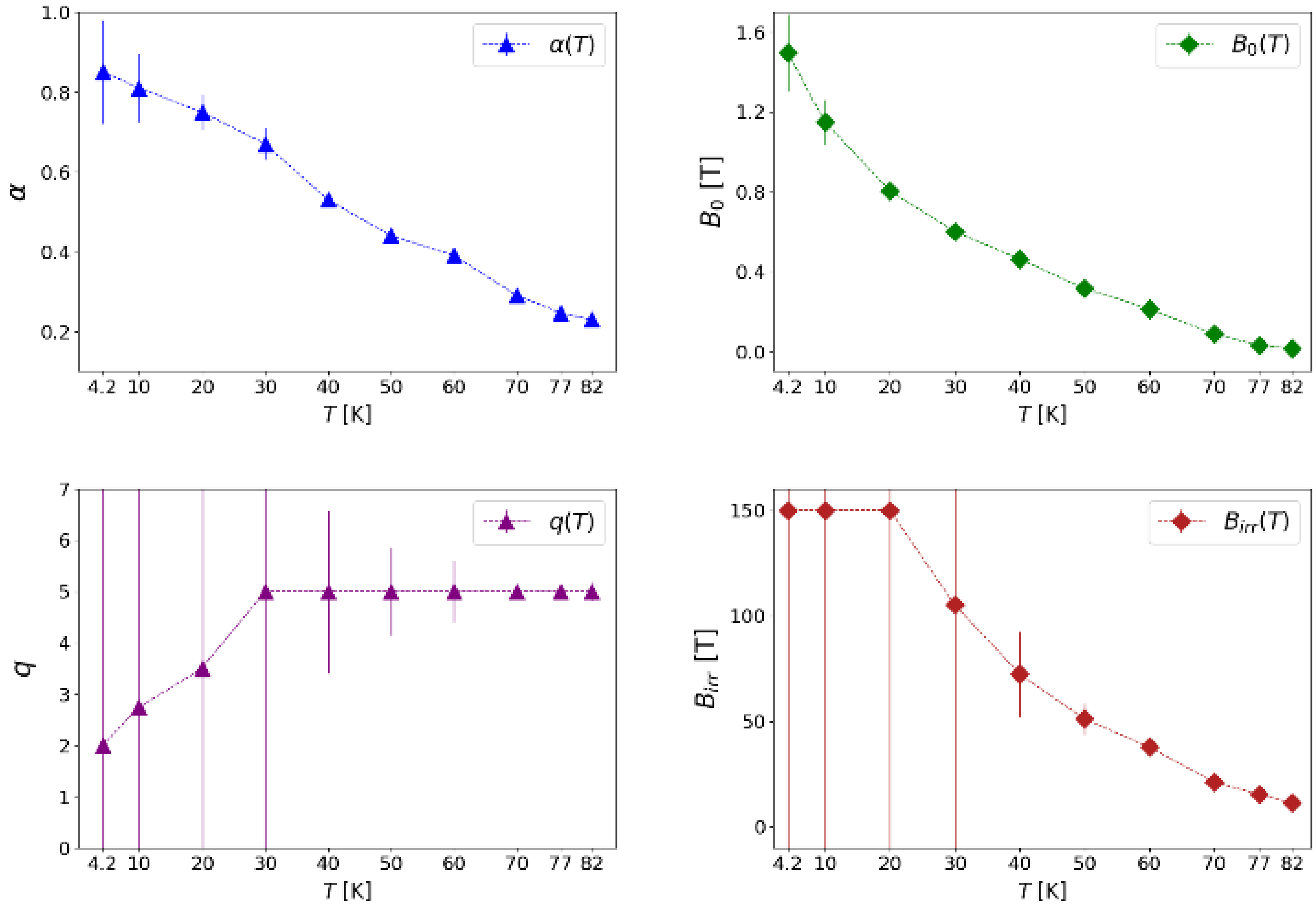

- *Note*: data are complemented by error bars, which here represent the standard deviation on the fitting, not the actual experimental error bars.

Temperature scaling

- The scaling can be extended to the temperature domain.

$$I_c(B, T = T^*, \theta = \theta^*) = I^*_{c,0} \cdot \left(1 + \frac{B}{B^*_0}\right)^{-\alpha^*} \cdot \left(1 - \frac{B}{B^*_{irr}}\right)^{q^*}$$

$$I^*_{c,0} = I_{c,0}(T^*) = I_{c,0,0} \cdot \left(1 - \frac{T^*}{T_c}\right)^{\gamma}$$

$$I_{c,0}(4.2\ K) = I_{c,0}(77\ K) \cdot \left(\frac{T_c - 4.2}{T_c - 77}\right)^{\gamma}$$

$$I_{c,0}(4.2\ K) = I_{c,0}(77\ K) \cdot (6.6)^{\gamma}$$

γ	$I_{c,0}(4.2K)/I_{c,0}(77K)$
1.2	9.6
1.3	11.6
1.4	14.0
1.5	17.0

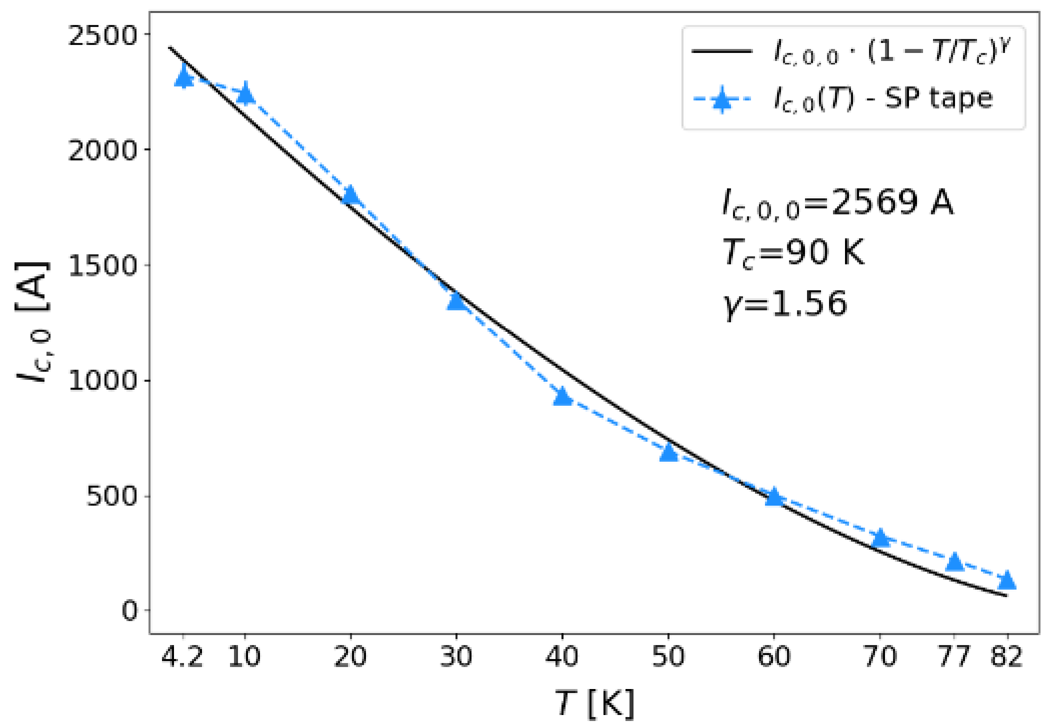

Outline

- REBCO properties and manufacturing routes
- Scaling laws
- Experimental activities
- Angular scaling
- Conclusions and next steps

Angular scaling - 1/4

- Due to mass anisotropy, $I_c(\theta)$ displays a sharp peak at 90°, namely in the direction parallel to the *ab*-planes.
- However, material inclusions can alter this picture, improving the overall performance (uncorrelated defects) and introducing peaks at specific angles (correlated defects).

J_c(77 K, 1 T) - Kang et al., 2007 , *modified from* [16]

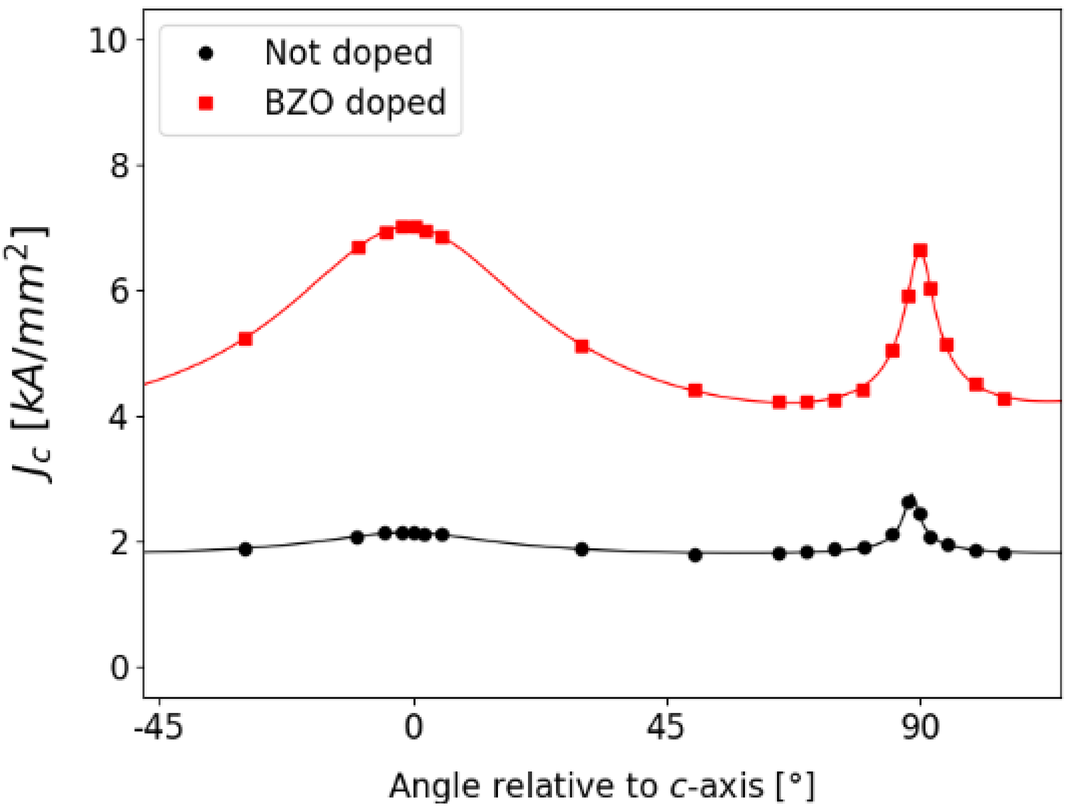

Angular scaling - 2/4

- We adopt the formulation from Hilton et al. [16]:

$$I_c(\theta) = I_0 + \sum_{k=1}^{n} I_{c,k} \cdot \frac{1}{\omega_k \cdot \varepsilon(\omega_k; \theta - \varphi_k)}$$

$$\varepsilon(\omega_k; \theta - \varphi_k) = \left[\cos^2(\theta - \varphi_k) + \frac{1}{\omega_k^2} \cdot \sin^2(\theta - \varphi_k)\right]^{\frac{1}{2}}$$

n	Number of peaks in the curve
$I_{c,k}$	Intensity of each peak
ω_k	Peak sharpness parameter
φ_k	Phase shift
I_0	Base value ($\omega_0 = 1$, common to all peaks)

J_c(77 K, 1 T) - Kang et al., 2007 [16]

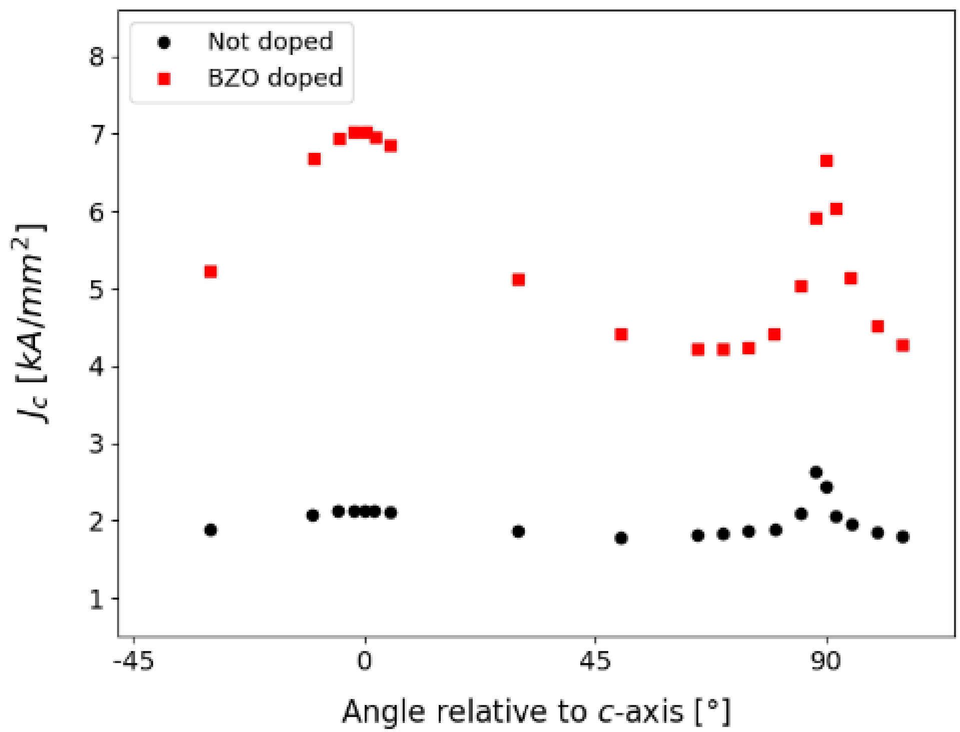

[16] S. Kang, et al., *Physica C: Superconductivity 457 41–6*, 2007.
[17] D. K. Hilton, A. V. Gavrilin, and U. P. Trociewitz, *Supercond. Sci. Technol., vol.28*, 2015.

Angular scaling – 3/4

In this case: $$I_c(\theta) = I_0 + I_{c,1} \cdot \frac{1}{\omega_1 \cdot \varepsilon(\omega_1; \theta - \varphi_1)} + I_{c,2} \cdot \frac{1}{\omega_2 \cdot \varepsilon(\omega_2; \theta - \varphi_2)}$$

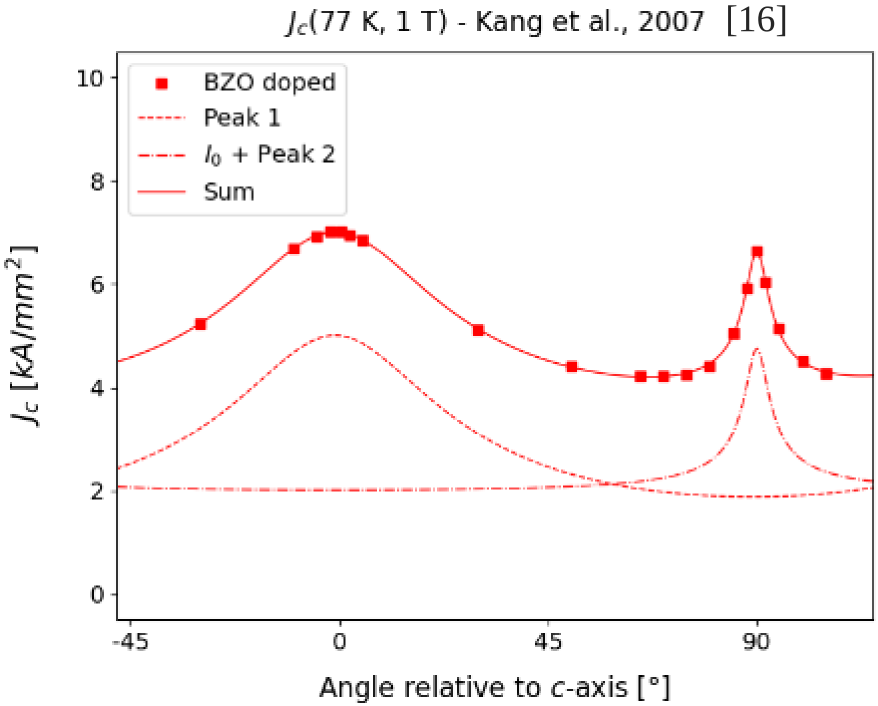

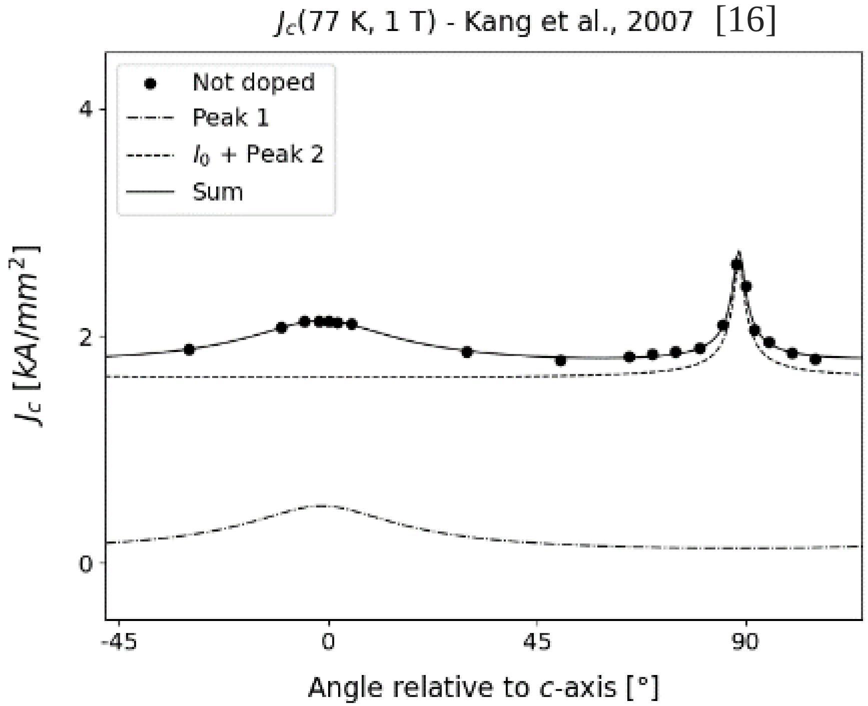

	I_0	$I_{c,1}$	ω_1	φ_1	$I_{c,2}$	ω_2	φ_2
Not doped	1.6	1.0	45.9	-1.5°	0.5	3.9	88.7°
BZO doped	1.9	2.9	23.4	0.0°	5.0	2.7	89.1°

[16] S. Kang, et al., *Physica C: Superconductivity 457 41–6*, 2007.

Angular scaling – 4/4

In this case: $$I_c(\theta) = I_0 + \sum_{k=1}^{4} I_{c,k} \cdot \frac{1}{\omega_k \cdot \varepsilon(\omega_k; \theta - \varphi_k)}$$

J_c(76 K, 5 T) - Civale et al., 2004 , *modified from* [18]

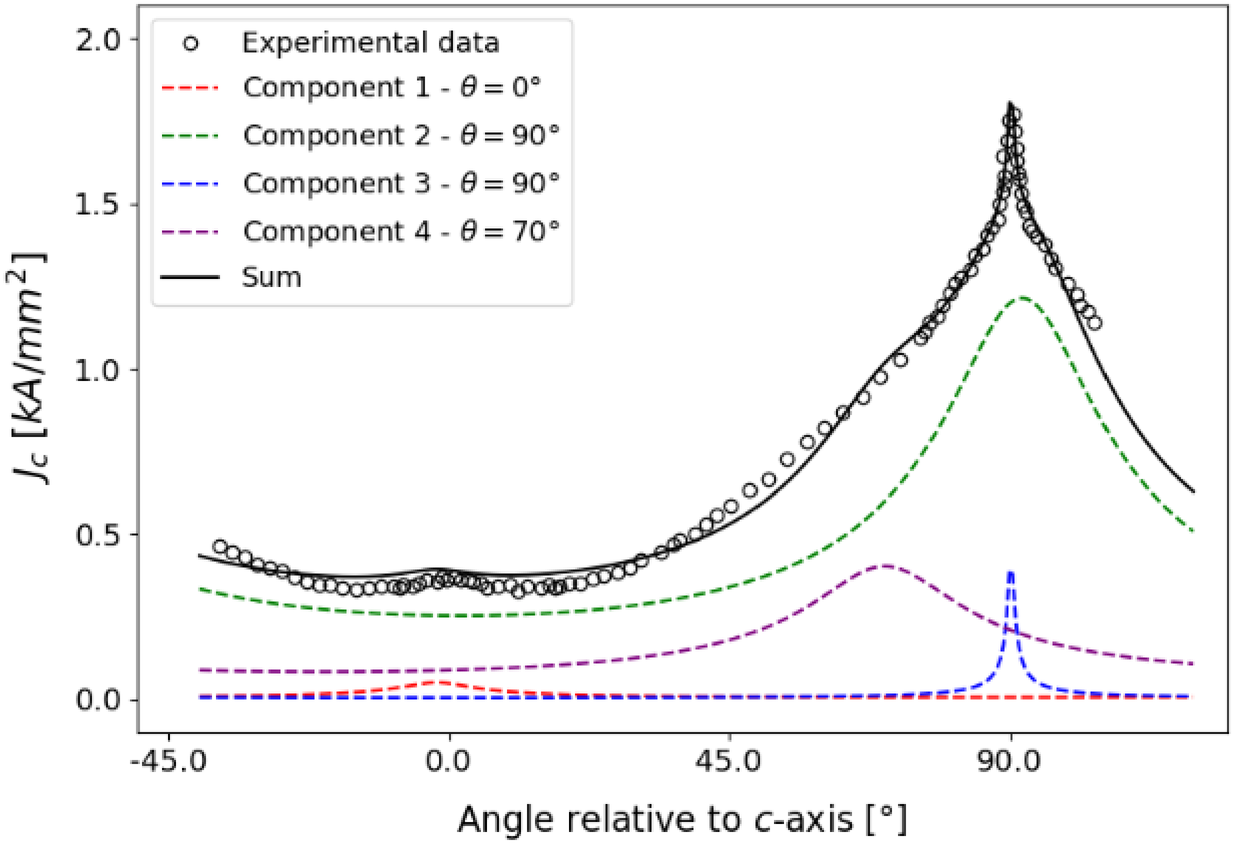

[18] L. Civale et al., *Physica C: Supercond.*, 2004

Outline

- REBCO properties and manufacturing routes
- Scaling laws
- Experimental activities
- Angular scaling
- Conclusions and next steps

Conclusion – 1/2

- REBCO is a quaternary complex material and its critical current, I_c, depends on the magnetic field intensity, B, temperature, T, and orientation angle, θ, of the magnetic field with respect to the tape, $I_c(B,T,\theta)$.

  Also, the I_c depends sensitively on the composition and nanostructure of the REBCO, which is determined by the *processing method and conditions*, such as supersaturation – the variation of concentration of the REBCO species from the equilibrium level.

- The full experimental characterization of the $I_c(B,T,\theta)$ of a tape over a wide field, temperature and angular domain is a complex and time-consuming procedure.

  Scaling laws are a fundamental tool to describe the dependence of tape performance from B, T, and θ. This is of the utmost importance for the design of coils and magnets.

Conclusion – 2/2

- The $I_c(B)$ is the combination of 3 regions (in a log-log plot), defining 3 different pinning regimes: single-vortex pinning, collective pinning, thermal activation.

- Past attempts at scaling laws aim mainly at *Region II* of the curve

⇩

Need to extend the description both to low fields, to compute magnetization and self-field effects in tapes, and to high fields.

- The scaling law proposed here covers the **entire field** (up to B_{irr}) **and temperature** (up to T_c) **spectrum**. It has been *validated* by means of both literature data and an experimental campaign using transport current as well as magnetization measurements on recent commercial tapes.

- An angular scaling proposed in the past has been applied to various sets of literature data, showing potential for further extension of our scaling law to the angular domain.

Next steps

- The purpose of this work is to build a database of scaling parameters for the manufacturers as well as to establish correlations with flux pinning enhancement mechanisms adopted by each manufacturer.

- The aim is to show that the scaling law combined with a few parameters, which are comprised in tight ranges for each manufacturing route, describes the entire $I_c(B,T)$ domain without requiring additional experimental effort from the magnet designer.

Thank you for your attention!

A special thanks to the technical team at Buildings 163 and 288 at CERN for the invaluable support in the experimental activities

References

[1] G. Succi, A. Ballarino, S. C. Hopkins, C. Barth, Y. Yang, “Magnetic field and temperature scaling of the critical current of REBCO tapes”, *IEEE Trans. Appl. Supercond.*, vol. 34, no. 3, 2024.

[2] E. Stilp et al., “Controlling the near-surface superfluid density in underdoped $YBa_2Cu_3O_{6+x}$ by photo-illumination”, *Scientific reports*, 2014.

[3] M. Cyrot and D. Pavuna, *Introduction to superconductivity and high-T_c materials*, World Scientific, 1992.

[4] A. Ballarino, Technical Superconductors: HTS, presented at CAS on Normal- and Superconducting Magnets, 2023.

[5] S. R. Foltyn et al., “Materials science challenges for high-temperature superconducting wire”, *Materials for Sustainable Energy* (Co-Published with Macmillan Publishers Ltd, UK) *pp 299–310*, 2010.

[6] J. Fleiter and A. Ballarino, “Parameterization of the critical surface of REBCO conductors at Fujikura”, *CERN EDMS document no. 1426239*, 2014.

[7] J. van Nugteren, “High temperature superconductor accelerator magnets”, *PhD thesis, Twente University*, 2016.

References

[8] M. Solovyov et al., *Supercond. Sci. Techn.*, vol. 26, no. 11, 2013.

[9] J. L. MacManus-Driscoll and S. C. Wimbush, “Processing and application of high-temperature superconducting coated conductors”, *Nature Reviews Materials*, vol. 6, 2021.

[10] A. Molodyk et al., “Development and large volume production of extremely high current density $YBa_2Cu_3O_7$ superconducting wires for fusion”, *Sci. Rep.*, vol. 11, 2021, Art no. 2084.

[11] E. J. Kramer, “Scaling laws for flux pinning in hard superconductors”, *J. Appl. Phys.*, vol. 44, no. 3, 1973.

[12] L. Bottura, “A practical fit for the critical surface of NbTi”, *IEEE Trans. Appl. Supercond.*, vol. 10, no.1, 2000.

[13] A. Xu et al., “Role of weak uncorrelated pinning introduced by $BaZrO_3$ nanorods at low temperature in $(Y,Gd)Ba_2Cu_3O_x$ thin films”, *Physical Review B*, 2012.

[14] C. Senatore et al. , “Field and temperature scaling of the critical current density in commercial REBCO coated conductors”, *Supercond. Sci. Techn.*, 2016.

References

[15] M. Daibo, “Recent progress of 2G HTS wires and coils at Fujikura”, *Workshop on Advanced Superconducting Materials and Magnets*, 2019.

[16] S. Kang, et al., “Flux-pinning characteristics as a function of density of columnar defects comprised of self-assembled nanodots and nanorods in epitaxial YBa2Cu3O7−δ films for coated conductor applications”, *Physica C: Superconductivity 457 41–6*, 2007.

[17] D. K. Hilton, A. V. Gavrilin, and U. P. Trociewitz, “Practical fit functions for transport critical current versus field magnitude and angle data from (RE)BCO coated conductors at fixed low temperatures and in high magnetic fields”, Supercond. Sci. Technol. 28, 2015.

[18] L. Civale et al., “Influence of crystalline texture on vortex pinning near the ab-plane in YBa2Cu3O7 thin films and coated conductors”, *Physica C: Superconductivity 412–414 976–82*, 2004.

Back-up slides

$I_c(\mathrm{B}, \mathrm{B}//\mathrm{tape})$: P-shape sample holder

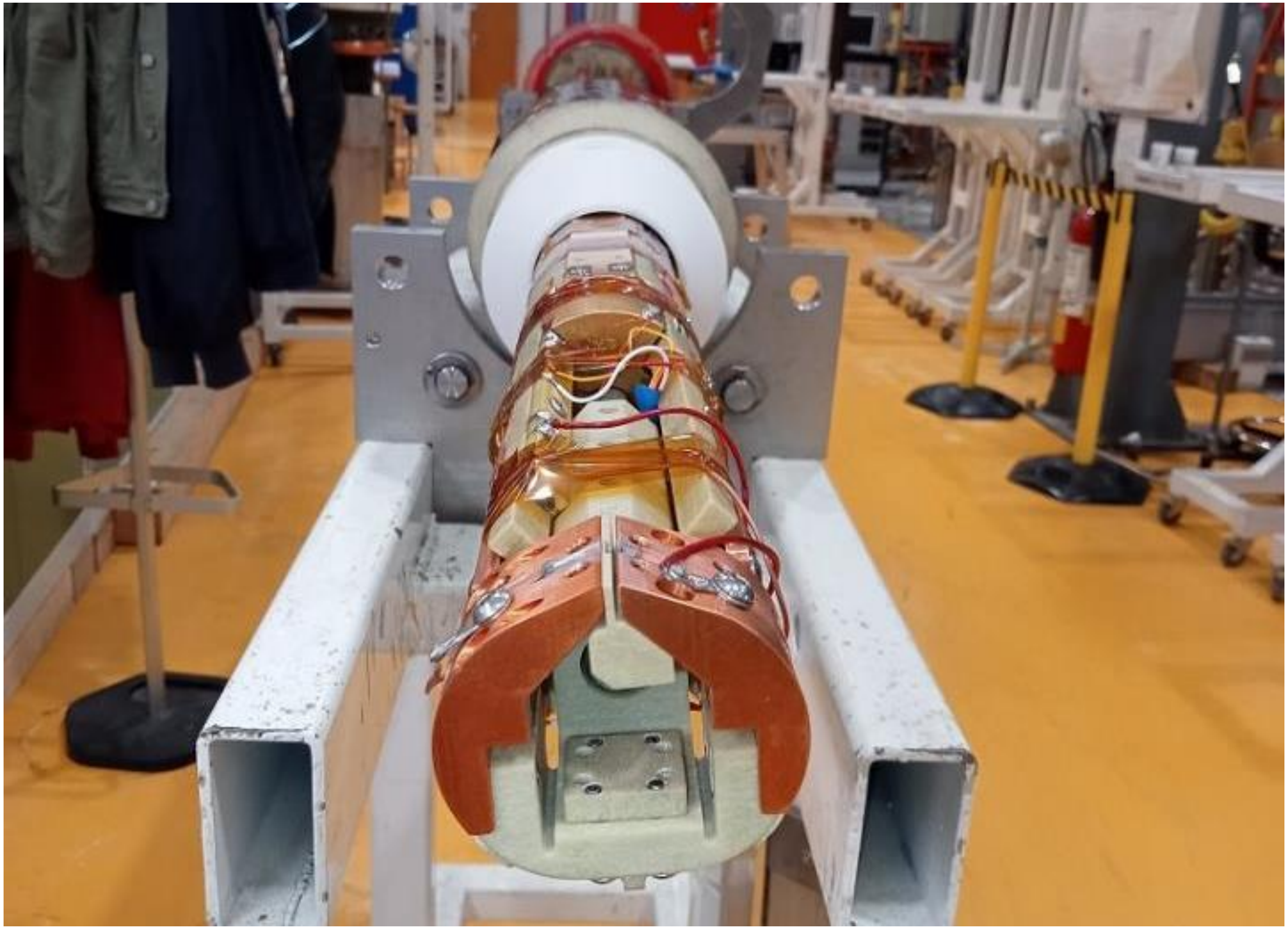

- Tape burnt at the end of testing – 26/3/2024

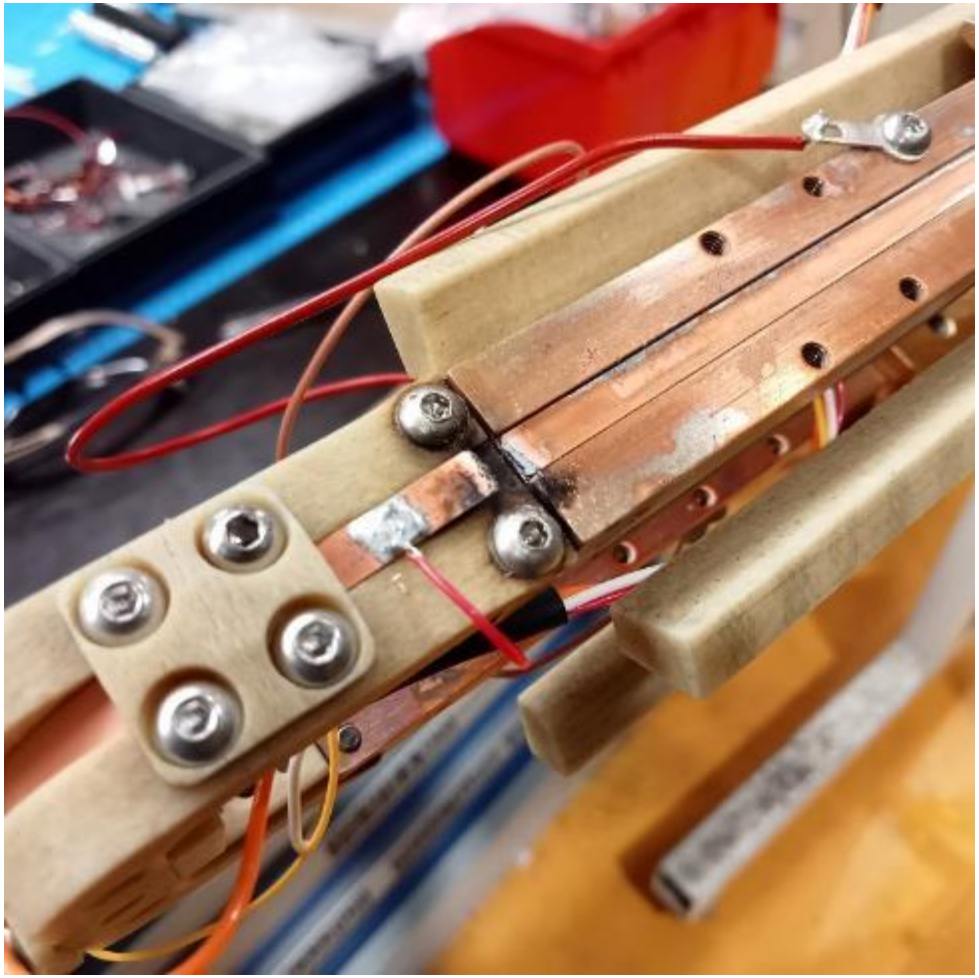

CERN

www.cern.ch